Enabling Resilient UK Energy Infrastructure: Natural Hazard Characterisation Technical Volumes and Case Studies

Case Study 2:

Dounreay

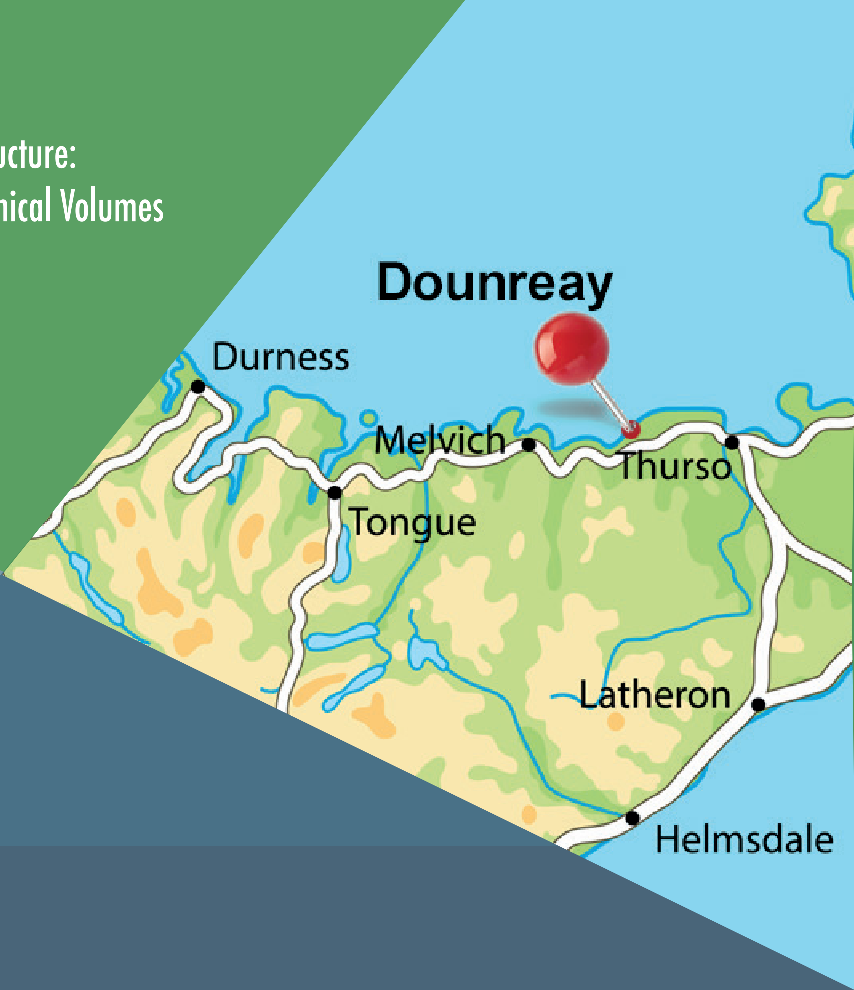

LC 0064_18CS2

EDF Energy · Energy Technologies Institute · IChemE Advancing Chemical Engineering Worldwide · Institution of Mechanical Engineers · Met Office · Mott MacDonald

Legal Statement

Authors: Tony Hull, Sun Yan Evans (Mott MacDonald); Kate Brown, Kate Salmon, Francis Colledge (Met Office); Angus Bloomfield (EDF Energy)
Chief Technical Officer: Hugo Winter (EDF Energy)

Version	Date	Details
0.1	05/04/18	Submitted for IPR
0.2	16/06/18	IPR comments addressed and submitted to CTO
1.0	28/06/18	CTO comments addressed and submitted to ETI
2.0	16/08/18	ETI and NHP3 Steering Committee comments addressed

This document forms part of the Energy Technologies Institute (ETI) project 'Low Carbon Electricity Generation Technologies: Review of Natural Hazards', funded by the ETI and led in delivery by the EDF Energy R&D UK Centre. The aim of the project has been to develop a consistent methodology for the characterisation of natural hazards, and to produce a high-quality peer-reviewed set of documents suitable for use across the energy industry to better understand the impact that natural hazards may have on new and existing infrastructure. This work is seen as vital given the drive to build new energy infrastructure and extend the life of current assets against the backdrop of increased exposure to a variety of natural hazards and the potential impact that climate change may have on the magnitude and frequency of these hazards.

The first edition of *Enabling Resilient UK Energy Infrastructure: Natural Hazard Characterisation Technical Volumes and Case Studies* has been funded by the ETI and authored by EDF Energy R&D UK Centre, with the Met Office and Mott MacDonald Limited. The ETI was active from 2007 to 2019, but to make the project outputs available to industry, organisations and individuals, the ETI has provided a licence to the Institution of Mechanical Engineers and Institution of Chemical Engineers to exploit the intellectual property. This enables these organisations to make these documents available and also update them as deemed appropriate.

The technical volumes outline the latest science in the field of natural hazard characterisation and are supported by case studies that illustrate how these approaches can be used to better understand the risks posed to UK infrastructure projects. The documents presented are split into a set of eleven technical volumes and five case studies.

Each technical volume aims to provide an overview of the latest science available to characterise the natural hazard under consideration within the specific volume. This includes a description of the phenomena related to a natural hazard, the data and methodologies that can be used to characterise the hazard, the regulatory context and emerging trends. These documents are aimed at the technical end-user with some prior knowledge of natural hazards and their potential impacts on infrastructure, who wishes to know more about the natural hazards and the methods that lie behind the values that are often quoted in guideline and standards documents. The volumes are not intended to be exhaustive and it is acknowledged that other approaches may be available to characterise a hazard. It has also not been the intention of the project to produce a set of standard engineering 'guidelines' (i.e. a step-by-step 'how to' guide for each hazard) since the specific hazards and levels of interest will vary widely depending on the infrastructure being built and where it is being built. For any energy-related projects affected by natural hazards, it is recommended that additional site- and infrastructure-specific analyses be undertaken by professionals. However, the approaches outlined aim to provide a summary of methods available for each hazard across the energy industry. General advice on regulation and emerging trends are provided for each hazard as context, but again it is advised that end-users investigate in further detail for the latest developments relating to the hazard, technology, project and site of interest.

The case studies aim to illustrate how the approaches outlined in the technical volumes could be applied at a site to characterise a specific set of natural hazards. These documents are aimed at the less technical end-user who wants an illustration of the factors that need to be accounted for when characterising natural hazards at a site where there is new or existing infrastructure. The case studies have been chosen to illustrate several different locations around the UK with different types of site (e.g. offshore, onshore coastal site, onshore river site, etc.). Each of the natural hazards developed in the volumes has been illustrated for at least one of the case study locations. For the sake of expediency, only a small subset of all hazards has been illustrated at each site. However, it is noted that each case study site would require additional analysis for other natural hazards. Each case study should be seen as illustrative of the methods outlined in the technical volumes and the values derived at any site should not be directly used to provide site-specific values for any type of safety analysis. It is a project recommendation that detailed site-specific analysis should be undertaken by professionals when analysing the safety and operational performance of new or existing infrastructure. The case studies seek only to provide engineers and end-users with a better understanding of this type of analysis.

Whilst the requirements of specific legislation for a sub-sector of energy industry (e.g. nuclear, offshore) will take precedence, as outlined above, a more rounded understanding of hazard characterisation can be achieved by looking at the information provided in the technical volumes and case studies together. For the less technical end-user this may involve starting with a case study and then moving to the technical volume for additional detail, whereas the more technical end-user may jump straight to the volume and then cross-reference with the case study for an illustration of how to apply these methodologies at a specific site. The documents have been designed to fit together in either way and the choice is up to the end-user.

The documents should be referenced in the following way (examples given for a technical volume and case study):

ETI. 2018. *Enabling Resilient UK Energy Infrastructure: Natural Hazard Characterisation Technical Volumes and Case Studies,* Volume 1 — Introduction to the Technical Volumes and Case Studies. IMechE, IChemE.

ETI. 2018. *Enabling Resilient UK Energy Infrastructure: Natural Hazard Characterisation Technical Volumes and Case Studies,* Case Study 1 — Trawsfynydd. IMechE, IChemE.

Contents

1. Introduction 7
   - 1.1 Site geography 7
     - 1.1.1 Introduction 7
     - 1.1.2 Landscape and geology 8
     - 1.1.3 Natural history and conservation 9
   - 1.2 Site oceanography 10
     - 1.2.1 Coastal zone 10
     - 1.2.2 Offshore environment 10
   - 1.3 Site climate 11
   - 1.4 Energy-related facilities 14
     - 1.4.1 Onshore installations 14
     - 1.4.2 Offshore installations 14

2. Characterisation of the natural hazards 16
   - 2.1 Extreme winds 16
     - 2.1.1 Extreme winds (excluding tornadoes) 16
     - 2.1.2 Tornadoes 23
     - 2.1.3 Minor hazards associated with extreme wind speed 31
   - 2.2 Extreme precipitation 32
     - 2.2.1 Definition 32
     - 2.2.2 Data 33
     - 2.2.3 Analysis 35
     - 2.2.4 Impact of climate change 38
     - 2.2.5 Minor hazards associated with rainfall 38
   - 2.3 Coastal/offshore flooding hazards 42
     - 2.3.1 Characterisation of offshore flooding hazards 43
     - 2.3.2 Monitoring and forecasting of waves 45
     - 2.3.3 Wave statistics near Dounreay 46
     - 2.3.4 Climate change consideration 48
   - 2.4 Biological fouling 48
     - 2.4.1 Characterisation of marine biological fouling 48
     - 2.4.2 Historical events and data 49
     - 2.4.3 Assessing the hazard 52
     - 2.4.4 Mitigation 53

3. Conclusions 55

References 58

Glossary 65

Abbreviations 67

Appendix A: EVA technique for extreme weather 68
- A.1 EVA 68
- A.2 Data requirements 69
- A.3 Advanced EVA for extreme daily rainfall including NAO covariate 72
  - A.3.1 Fitting a PP-GPD model that includes a covariate for the NAO 72
  - A.3.2 Further considerations 74

Appendix B: Wave graphs from WaveNet 76

Appendix C: Species data for Dounreay 80

1. Introduction

This case study illustrates the appropriate use of the derived methodology for assessing the risks of natural hazards that may arise in the Dounreay area, which is located on the north coast of Scotland. Dounreay is home to onshore nuclear installations and offshore renewables testing facilities. The land in the area near Dounreay is exposed and vulnerable to natural hazards from the sea (specifically from the North Atlantic towards the west and the North Sea towards the east). Thus, Dounreay can be taken to represent both coastal (onshore) and offshore sites.

Aspects of four different types of natural hazards are addressed in this case study:

- Volume 3 — Extreme Wind — onshore effects;
- Volume 4 — Extreme Precipitation — onshore effects;
- Volume 6 — Coastal Flooding — offshore effects;
- Volume 11 — Marine Biological Fouling — offshore effects.

For extreme wind and precipitation, the case study focuses on onshore data but also recognises potential offshore impacts. The assessment of coastal flooding and marine biological fouling hazards are illustrated for the offshore environment here. An assessment of onshore marine biological fouling is provided in Case Study 3 — Hunterston, and an assessment of onshore coastal flooding is provided in Case Study 4 — Teesmouth.

The methodologies applied for each hazard are described in the individual technical volumes associated with each of the hazard families.

1.1 Site geography

1.1.1 Introduction

Dounreay is located in the Scottish Highlands (*Figure 1*) in the historic county of Caithness, which is in the Highland Council area. Dounreay is served by a dedicated access road running north from the A836, approximately 13 kilometres (km) west of Thurso. The A836 provides the main east-west link along Scotland's north coast; it passes to the south of the Dounreay site and connects to the A9. Thurso has a railway station which links to the UK rail network. There is a small airport at Wick with scheduled services to other UK airports. The Dounreay site also has a private airstrip. Nearby Scrabster harbour acts as the main ferry port for the Orkney Islands and as a commercial port for major subsea service contractors, located at the Atlantic frontier. Investments in infrastructure at Scrabster mean that large offshore vessels can now access the port at any tide.

In 2011, the population of Caithness was 26,486, representing around 11.4% of the total population of the Highland Council area (*NDA, 2014*).

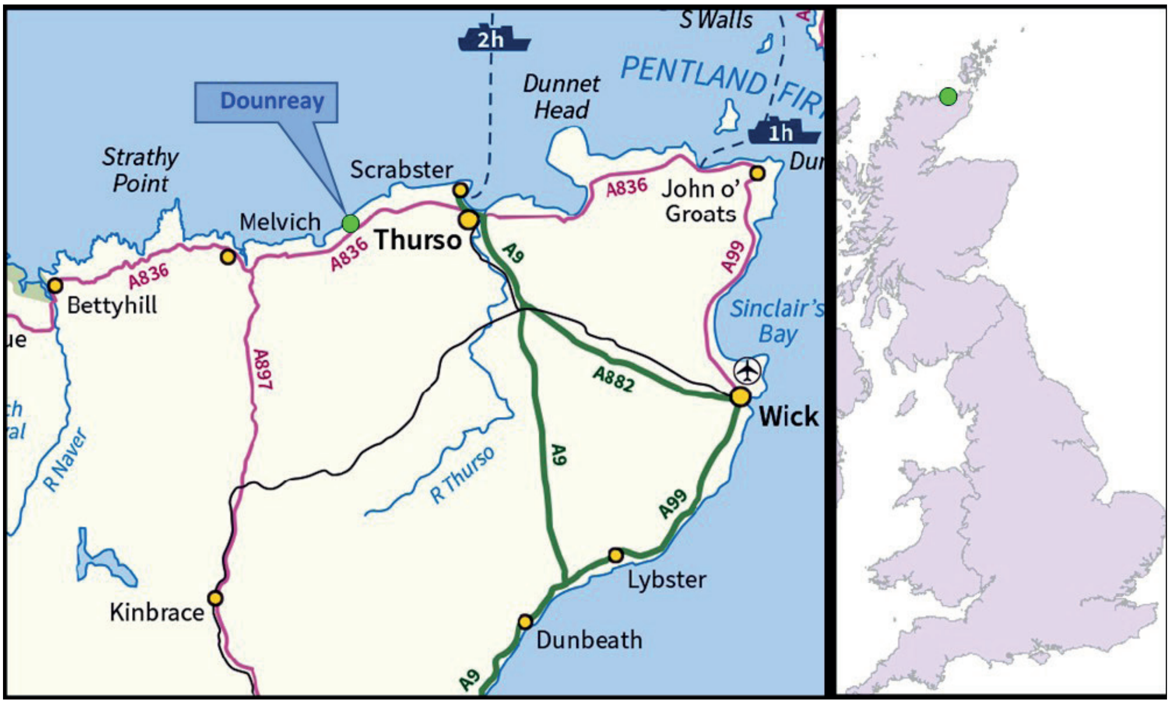

Figure 1. Location of Dounreay in the Scottish Highlands
(Source: contains OS data © Crown Copyright and database right (2018))

1.1.2 Landscape and geology

The coastline around Dounreay consists of predominantly rocky shores backed by cliffs, interrupted by the occasional sandy beach. While most of the coastlines in Highland are considered underdeveloped and isolated, Dounreay is considered a developed coast, based on certain primary and secondary indicators (*The Highland Council, 2010*).

The Dounreay nuclear site divides a strip of farmland, situated between the north coast of Caithness and the main coast road, the A836. The region is generally flat, characterised by open rolling countryside with hills west and south. The majority of the Dounreay site is located approximately 20 m above *ordnance datum** (AOD).

Dounreay is a coarse sandy shingle site, underlain by rocks of the Caithness Flagstone Formation. These are predominantly grey siltstones with minor sandstones and limestones. The rocks are indurated (hardened) with very low porosity. Overlying Quaternary deposits are generally greater than 3 m thick. No geological features of special importance have been identified. The

*All technical terms marked in blue can be found in the Glossary section.

solid strata and overlying deposits at the site are typical of the much wider area and, as such, there are no scarce or locally restricted deposits of note.

Much of the coastline experiences a tidal rise and fall of around 1.7 metres (m) (*Jones, 1975*). Coastline recession rates of around 1 to 2 m in 200 to 300 years have been estimated, taking into account sea level rise (*NDA, 2014*). In the longer term, parts of the site will be more susceptible to sea level rise and coastal erosion over timescales of several hundred to thousands of years, if no additional mitigation measures are applied.

Groundwater in some small areas of the site is known to be impacted by radioactive contamination. Control measures are in place for this and are authorised as necessary by the Scottish Environment Protection Agency (SEPA). Localised contamination of groundwater by industrial solvents is being investigated. No groundwater flooding was shown on this site in SEPA's flood maps (*SEPA, 2018*).

1.1.3 Natural history and conservation

There are no designated conservation sites identified on the Dounreay nuclear site. There are, however, Sites of Special Scientific Interest (SSSIs), Special Areas of Conservation (SACs), Special Protection Areas (SPAs), Ramsar sites, and Ancient Woodland Inventory (AWI) sites in the surrounding area.

A number of protected species were recorded on, or next to the site, including otters (European protected species under Annex IV of the Habitats Directive) and breeding birds, such as the Arctic tern. Species of flora including the nationally uncommon oyster plant and Scottish primrose are found on the Dounreay beach. The north coast of Scotland is home to some of the rarest species of bee in the UK including the great yellow bumblebee and the moss carder bee (a UK Biodiversity Action Plan priority species).

A river, the Dounreay Burn (also known as the Mill Lade) flows through the Dounreay site and is considered as being of good quality status in accordance with the Water Framework Directive (*European Commission, 2000*). The coastal waters around Dounreay are also considered to be of high quality status in relation to the Water Framework Directive. Seawater and sediment samples have been collected and analysed, and they support this statement.

1.2 Site oceanography

1.2.1 Coastal zone

The coastal zone in the region of Dounreay mainly consists of shallow bays and estuaries, and long stretches of coastline that have little shelter from waves and storms. The north coastlines are predominantly rocky but there are intertidal sediments in the bays and inlets, and some extensive stretches of sandy beach. The coastline of the Western Isles, the north of Scotland and the Northern Isles is also rocky. The west coast is typically rocky, with many bays, channels and sea lochs where restricted water exchange occurs with the surrounding seas. There are high levels of freshwater input from rivers, particularly into the sea lochs.

1.2.2 Offshore environment

The shoreline of the north coast of Scotland opens onto an extensive offshore environment. The Orkneys lie a little over 30 km away to the north-east across the Pentland Firth, with the Shetlands located beyond them. The expanses of the North Sea stretching east across to Norway and the North Atlantic Ocean to the west are dominant features of the offshore environment in this area. Scotland's seas are some of the most diverse in physical characteristics on the planet. They are at the confluence of northerly-flowing surface currents and southerly-flowing polar currents and the complex *bathymetry* to the west causes these to become mixed, bringing nutrients to the surface. These are fed on by plankton communities which form the basis for a rich fishing region.

The offshore environment in Scottish waters ranges from shelf sea areas to deep ocean regions with depths greater than 2000 m (*Scottish Government, 2011*). Average water depths vary but are generally between 50 m and 200 m for the shelf seas, typically between 100 m and 150 m to the west of the Hebrides and off the north coast; the waters being generally shallower around the south-west area of Scotland.

The continental shelf includes the Malin and Hebrides Shelf Seas, Orkney and Shetland Shelf Seas, and the North Sea. The western margin of the continental shelf is marked by a sharp change in depth of the seabed at about 200 m. The main offshore habitats on the west coast are coarse sands, gravel and rock. To the west of the Outer Hebrides and to the north of Scotland the main offshore habitats are expanses of mud, sand and coarse sediment. In the deeper waters to the west and north of Scotland, the main habitats are large expanses of mud and fine clay, but a variety of coarse sediments are found in shallow waters, on banks and seamounts. Sea levels are affected over short timescales by the rise and fall of the tide and storm surges. Over longer timescales, the sea level is affected by climate change and movements of land. Tidal range is generally between 4 m and 5 m.

Within Scottish waters, the wave climate is mainly influenced by the conditions in the North Atlantic Ocean, where the fetch is long enough to establish large swell waves.

1.3 Site climate

Dounreay experiences a maritime climate much like the rest of the UK, as demonstrated by the annual climatologies of temperature, rainfall and wind shown in *Figure 2* and *Figure 3*. Typically, the climatology (long-term averages representative of the climate) of a region is defined by averaging variables such as temperature and rainfall over a 30-year baseline period. In this case, temperature and rainfall for Dounreay and two additional weather stations nearby (Wick Airport and Kirkwall; see map in *Figure 12*) are shown for the 1961 to 1990 period. Dounreay weather station stopped recording data in 1983 so, where possible, missing temperature and rainfall data have been estimated using linear regression from overlapping data periods with up to six well-correlated neighbouring weather stations (*Perry and Hollis, 2005*). Ideally, a more recent 30-year climatology (e.g. 1981 to 2010) would be used, but this would then only consist of two years of observed data for Dounreay, with the remaining 28 years being estimated from neighbouring sites. To allow comparison between the sites, the wind roses shown in *Figure 3* for Wick Airport and Kirkwall are restricted to the same period of operation as Dounreay (1969 to 1983). Local weather extremes for the Dounreay site are also provided in *Table 1*.

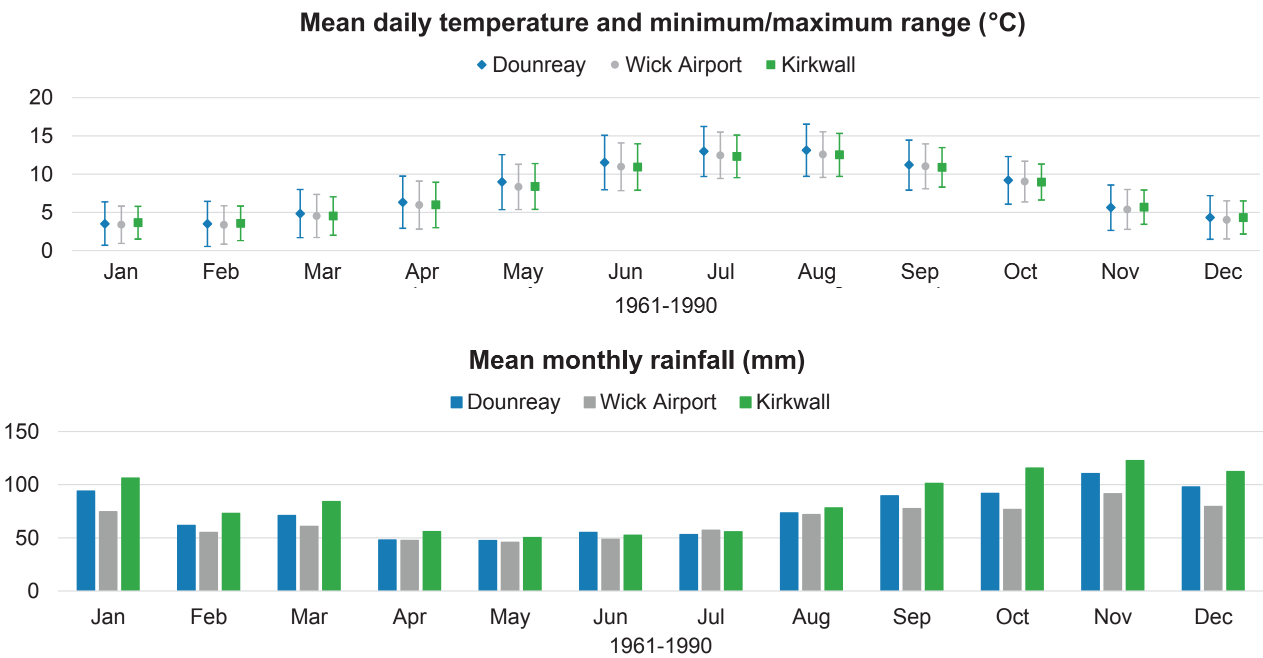

Figure 2. Climatology of daily mean, minimum and maximum temperatures and of monthly rainfall for the weather stations indicated on the graphics, for the period of 1961 to 1990. Missing data for Dounreay (from 1983) were estimated (where possible) using a linear regression from overlapping data periods with up to six well correlated neighbouring weather stations following the approach of Perry and Hollis (2005).

Figure 2 shows that July and August are the warmest months at Dounreay with a mean daily temperature of approximately 13 degrees Celsius (°C) (mean daily maximum temperature of approximately 16 °C). January and February are the coldest months with a mean daily temperature of approximately 6 °C (mean daily minimum temperature of approximately 1 °C).

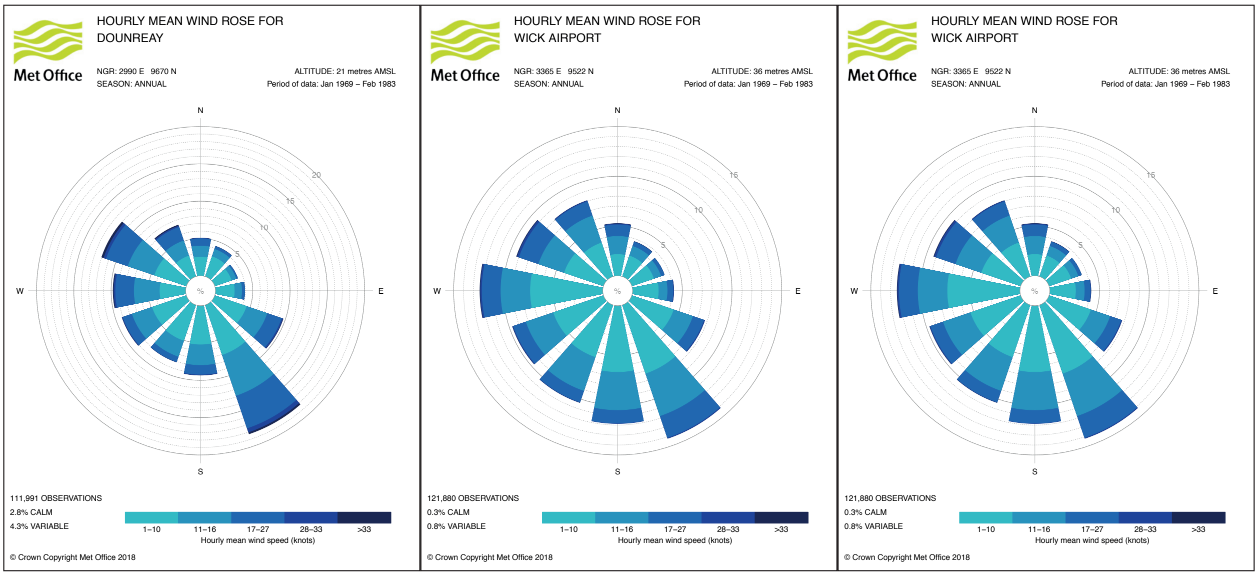

Figure 3. Climatology of wind speed and direction for Dounreay, Wick Airport and Kirkwall weather stations for the period of 1969 to 1983.

Caithness lies to the east of higher grounds and as a result, its annual rainfall totals are much smaller than those of western Scotland. Across Caithness, annual average rainfall (from 1981 to 2010) ranges from 800 millimetres (mm) to 1000 mm in the east and northern coastal regions, to 1000 to 1250 mm to the west and south. Rainfall is generally well distributed throughout the year, but there is a marked seasonal variation. The frequency of Atlantic depressions affecting Scotland is normally greatest during the winter, but Scotland tends to remain under their influence for much of the summer too. Caithness experiences an autumn and early winter maximum in rainfall totals, with spring and summer being the drier seasons on average. Autumn and winter are wetter than the spring and summer and Dounreay receives more rainfall on average than Wick Airport. It is likely this stems from the location of Wick Airport which is sheltered from the prevailing south-westerly wind direction and associated frontal rainfall. In contrast, Kirkwall, situated in Orkney to the north-east of Dounreay, is more exposed to the prevailing wind direction and frontal rain, and is generally wetter than both Dounreay and Wick Airport.

The prevailing wind direction in the UK is typically from a south-westerly direction, as demonstrated by the wind roses for Kirkwall and Wick Airport. However, the dominant winds at Dounreay originate from south-easterly and north-westerly directions. One possible explanation for this difference is that Dounreay is sheltered from the prevailing south-westerly winds by the higher ground located to the south-west. However, despite being surrounded by different topography, the maximum recorded hourly mean wind speeds at Dounreay, Wick Airport and Kirkwall, for 1969 to 1983, are all similar with hourly mean wind speeds greater than 33 knots (17 metres per second (m/s) or 38 miles per hour (mph); 1 knot = 0.51 m/s = 1.15 mph).

Ground frost, defined as a minimum grass temperature below 0 °C, typically occurs from November to April with over half the days in the month being frost days between December and February. However, frosts can be observed as early as September and as late as June and within the record there is an observation of a frost event occurring both in July and August. Much of the snow that falls does not settle, and as a result several different parameters on snowfall can be reported. These include snow depth, whether snow was observed falling during the day, and whether snow was observed laying on the ground at 09:00 Greenwich Mean Time (GMT). For Dounreay, snow was observed on the ground at 09:00 between November and March and there were two occasions of snow on the ground outside of these months; one in April and the other in May. Between years, there is considerable variability in the number of days when snow is observed on the ground: Seven years had no snow events and six years had more 15 or more days of snow laying. The largest number of days in a year when snow was recorded on the ground was 27.

Table 1. Local weather extremes at Dounreay. Records are available for temperatures and snow (1959 to 1983), rainfall (1961 to 1983), and daily wind speed (1969 to 1983). (© Crown Copyright Met Office 2018)

Dounreay	Value	Date
Temperature		
Highest daily temperature	28.9 °C	12th August 1975
Lowest daily temperature	–10.6 °C	30th December 1961
Rainfall		
Maximum daily rainfall total	62.5 mm	17th August 1964
Maximum daily snow depth	230 mm	16th February 1970
Wind speed		
Maximum daily wind speed	40 knots	2nd March 1970

1.4 Energy-related facilities

1.4.1 Onshore installations

Once the site of a castle, Dounreay has been home to nuclear research establishments (including the Dounreay Nuclear Power Development Establishment and the Vulcan Naval Reactor Test Establishment) since the 1950s; many of these facilities have now been, or are in the process of being, decommissioned. The nuclear facilities at Dounreay are no longer capable of producing power and the site's concerns are now construction, demolition and waste management as part of the major decommissioning and clean-up programme to convert the site to a brownfield site. One of the power stations at Dounreay is situated close to the coast, it has a high water table, and the station uses a pump to constantly remove water. For these reasons, a requirement for a secondary flood defence solution was identified by the Dounreay Site Restoration Ltd, the licence company responsible for the clean-up and decommissioning of the nuclear power stations.

The Highlands and Islands of Scotland have a long history in the oil and gas sector and, over the past 40 years, have played a pivotal role in the development of the Scottish oil and gas industry. Orkney has strong historical links to the energy industry and the Flotta oil terminal operates as the second largest major oil terminal serving the UK North Sea, and has provided a landing for the Piper and Claymore fields' pipeline system. The ports of Kirkwall, Stromness and Lyness have seen significant investment to continue to provide facilities for the oil and gas industry as well as the marine renewables industry.

1.4.2 Offshore installations

The Pentland Firth and Orkney waters are among the most active tidal areas in the world and the commercial lease area hosts six of the top ten tidal energy sites in the UK. It is also home to the European Marine Energy Centre (EMEC) which provides testing facilities to the marine renewable energy industry, and includes the tidal stream project, MeyGen, the first phase of which became commercially operational in April 2018. This area of the sea contains 50% of the UK's tidal resource and 25% of Europe's tidal resource (*HI-energy, 2018*).

Wave energy is mainly at the development phase; however, consistent and committed support from the Scottish Government indicates that wave energy is seen as being a significant contributor to Scotland's electricity requirements (*Scottish Government, 2017*).

Scotland as a whole makes up around 25% of the whole European offshore wind resource and the world's first deep water offshore wind project has been operating some 15 miles off Caithness, in 45 m of water. The Beatrice wind farm demonstrator project has seen the design, construction, installation and operation of two 5 megawatt (MW) turbines, 234.5 m from seabed to blade tip. Linked by subsea cable to the nearby Beatrice Alpha platform, they are generating 30% of the Beatrice Alpha oil platform's 14 MW daily electricity requirement (*HI-energy, 2018*).

Four types of natural hazard are considered in this case study for Dounreay. They are extreme wind, extreme precipitation, coastal flooding (including offshore flood-related hazards) and marine biological fouling. Extreme wind and precipitation hazards are considered for the onshore environment, whereas 'coastal' flooding and marine biological fouling hazards are focused on the offshore environment.

For background information, the reader should refer to the corresponding technical volumes:

- Volume 3 — Extreme Wind;
- Volume 4 — Extreme Precipitation;
- Volume 6 — Coastal Flooding;
- Volume 11 — Marine Biological Fouling.

2.1 Extreme winds

This section covers the analysis of extreme wind speed using extreme value theory and tornadoes using a database of tornado occurrences for the UK provided by the Tornado and Storm Research Organisation. The occurrence of sandstorms is also briefly mentioned.

2.1.1 Extreme winds (excluding tornadoes)

Definition

Wind speed is typically measured using an anemometer and recorded in knots (nautical mile per hour = 0.51 m/s) at Met Office observation stations. Wind speed and associated damage is categorised on the Beaufort scale which traditionally describes wind intensity based on observed sea conditions. Equally, the Saffir-Simpson Hurricane Wind scale can be used to define tropical cyclones. However, there is no such defined categorisation for land-based surface winds. The definition of an extreme wind speed event for the energy sector and of any associated wind speed threshold will differ depending on the type of asset, its vulnerability and exposure.

Extreme wind speeds and especially gusts (as defined in Volume 3 — Extreme Wind) can directly interfere with the generation of energy, energy transmission and distribution through destruction of infrastructure, as well as posing health and safety concerns for energy businesses. Furthermore, impacts from this disruption could have implications for energy demand and price. The dominant impacts are briefly outlined below:

- damage to power lines or energy infrastructure from fallen debris or trees causing extensive power cuts;
- injury or death from debris and fallen trees;

- structural damage to buildings, e.g. tiles blowing off roofs or impact on roofs by wind-blown debris;
- disruption to transport, e.g. through the closure of roads and bridges, and delays and cancellations to trains and aircraft, which in turn can affect the accessibility of sites to maintenance crews.

Typically, faster wind speeds are found in areas with few surrounding obstacles that would cause friction in the air, for example at higher altitudes, in open country or over water, as opposed to in urban environments with high-rise buildings and trees. This makes Dounreay a particularly exposed site as it is adjacent to the sea and surrounded by an expanse of flat land. Dounreay is also located in the most northern part of Scotland which is more at risk from extreme wind storms because damaging wind gusts typically increase with latitude in the UK (*Hewston and Dorling, 2011*).

Data

Wind characteristics typically recorded at an observing site include daily and hourly mean wind speed, prevailing hourly wind direction and maximum gust speeds (typically defined as the highest wind speed sustained for at least three seconds occurring over a defined period, e.g. an hour). Gust speeds are useful to characterise potential damage to infrastructure (*Prahl et al., 2015*); however they are often not recorded as consistently as daily mean wind speeds. If gust data are required but are not available at a particular site, then analytical relationships can be used to derive the gusts from hourly mean wind speeds, provided that the latter are available (*Ashcroft, 1994*).

In this case study, daily mean wind speeds are used to characterise extreme wind speeds at Dounreay and no account is taken of the wind direction or gusts. The reader should note that the extreme value analysis (EVA) techniques applied here could equally be applied to a sufficiently long time-series of hourly mean wind speeds or to gusts.

The top ten daily mean wind speeds recorded at weather stations closest to Dounreay are shown in *Table 2*. Dounreay's wind record being too short, Kirkwall was selected as the most suitable alternative weather station to Dounreay, from all the weather stations described in *Table 2* (i.e. the station with the smallest mean squared deviation as per the approach described in *Appendix A*).

The importance of the geographical location of the weather stations is also apparent in the table. Weather stations located further to the west experience stronger wind speeds (e.g. Stornoway Airport versus Wick Airport). Sule Skerry (not shown) is more exposed and experiences greater wind speeds because lesser surface friction over water means that mean wind speeds at this weather station are generally greater than over land for the same pressure gradient (*Raynor, 1978*). At seasonal timescales, both Dounreay and Kirkwall experience the highest daily mean wind speeds during winter and the lowest wind speeds during summer.

Table 2. The top ten daily mean wind speeds at the weather stations closest to Dounreay. The period over which these apply are the operation periods of each individual weather station (Dounreay = 1969 to 1983, Kirkwall = 1969 to present, Wick Airport = 1965 to present, Stornoway Airport = 1957 to present). Days where extremes occur at more than one site are numbered between 1 and 5. (© Crown Copyright Met Office 2018)

Rank	Top 10 windiest days at Dounreay		Top 10 windiest days at Kirkwall		Top 10 windiest days at Wick Airport		Top 10 windiest days at Stornoway Airport	
	Date	Daily mean wind speed, m/s (knots)	Date	Daily mean wind speed, m/s (knots)	Date	Daily mean wind speed, m/s (knots)	Date	Daily mean wind speed, m/s (knots)
1	2nd Mar 1970	20.6 (40)	[4]19th Sep 1990	21.6 (42)	4th Feb 1999	19.0 (37)	16th Feb 1962	25.7 (50)
2	1st Mar 1970	20.1 (39)	[5]29th Jan 2000	21.6 (42)	[4]19th Sep 1990	18.5 (36)	2nd Jan 1964	23.2 (45)
3	[1]28th Sep 1969	19.5 (38)	5th Jan 1975	21.1 (41)	5th Apr 1967	18.0 (35)	23rd Dec 1963	22.6 (44)
4	[2]18th Jan 1972	19.5 (38)	4th Feb 1999	21.1 (41)	[1]28th Sep 1969	18.0 (35)	24th Dec 1963	22.1 (43)
5	11th Oct 1981	19.5 (38)	[2]18th Jan 1972	20.1 (39)	28th Jan 1978	18.0 (35)	26th Jan 1961	21.6 (42)
6	12th Oct 1981	19.5 (38)	9th Jan 1983	20.1 (39)	22nd Jan 1985	17.5 (34)	15th Feb 1962	21.6 (42)
7	3rd Mar 1972	19.0 (37)	17th Jan 1993	20.1 (39)	3rd Apr 1998	17.5 (34)	20th Nov 1959	21.1 (41)
8	27th Oct 1974	19.0 (37)	25th Nov 2005	20.1 (39)	[5]29th Jan 2000	17.5 (34)	24th Oct 1961	21.1 (41)
9	17th Jan 1972	18.5 (36)	[3]20th Jan 1976	19.5 (38)	[3]20th Jan 1976	17.0 (33)	17th Dec 1966	20.6 (40)
10	[3]20th Jan 1976	18.5 (36)	5th Jan 1993	19.5 (38)	3rd Jan 1984	17.0 (33)	31st Jan 1958	20.1 (39)

Analysis

The aim of the following analysis is to estimate return levels of extreme winds using the generalised extreme value (GEV) approach (see *Appendix A*).

Selecting extreme maximum daily wind speeds

A GEV model is typically fitted to block maxima, i.e. the maximum daily wind speeds for each year for Kirkwall in this case. Data from the Met Office archive are automatically quality-controlled, but a further look at the values is necessary to ensure that they are as accurate as possible. *Figure 4* shows a time series of maximum daily wind speed for each month for Kirkwall.

The maximum daily wind speeds for each month for Kirkwall appear realistic. Values are within the range of maximum daily wind speeds recorded in the UK. The maximum value ever recorded is 39 m/s at Cairngorm Summit (altitude 1237 m) on 20th March 1986. At more low-lying weather stations (altitude under 100 m), the highest daily mean wind speed recorded is 26 m/s at the Isle of Wight (altitude 80 m) and Stornoway (altitude 15 m).

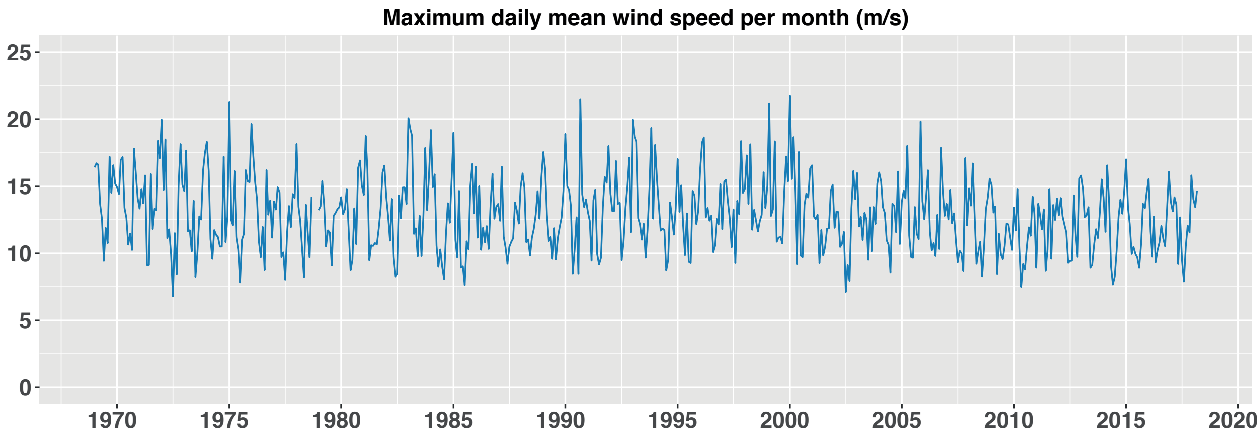

Figure 4. Maximum daily mean wind speed at Kirkwall for each month from January 1969 to March 2018 (© Crown Copyright Met Office 2018)

An EVA can be affected by missing values. Missing values could be ignored, for example by extracting the maximum daily mean speed value regardless of the number of missing days of observations in a year. This approach could however lead to an underestimation of return levels in the EVA. Any year with a missing value could alternatively be ignored in the selection of maximum daily mean speed values, but this would reduce the number of observations available and could cause problems in obtaining a well-fitting GEV model as the sample of extreme events becomes small. The latter approach would be less likely to underestimate return levels but the uncertainty associated with the return levels and the confidence intervals would be larger.

In this case study a hybrid approach was adopted. Any year containing a month with more than five missing values was excluded. However, for months containing fewer than five missing values, it was assumed that the windiest day of the month did not occur on a missing day. This approach resulted in the exclusion of the following years from the analysis: 1978, 2001, 2002, 2004, 2008, 2012 and 2018. As a result, the set of extreme values consisted of 42 maximum daily mean wind speeds.

Fitting a GEV model

Once the quality of the data has been assessed, and the annual extremes extracted, a GEV distribution can be fitted.

A GEV distribution is characterised by three parameters: location, scale and shape. For the Kirkwall data, the estimated location, scale and shape parameters obtained from the fit are listed in *Table 3*. Parameter values have an uncertainty (a sampling error associated with them which arises because they are derived from a sample of data). Parameter estimates would change if more data, or if a slightly different set of data, were available.

Table 3. Estimated location, scale and shape parameters of the fitted GEV distribution to the annual largest mean wind speed observed in the period 1970 to 2017.

	Location	Scale	Shape
Estimated value	16.88	1.71	–0.13
Standard error	0.31	0.23	0.13
95% normal-approximated confidence interval	[16.27, 17.48]	[1.27, 2.16]	[–0.41, 0.14]
95% profile-likelihood confidence interval	[16.32, 17.49]	[1.29, 2.18]	[–0.34, 0.21]

The standard error is a statistic that can be used to quantify the size of the change. A 95% confidence interval gives an estimated range of values which has a probability of 0.95 that it contains the true, unknown parameter estimate. As described in Section 4 of Volume 3 — Extreme Wind, the profile-likelihood method for calculating confidence intervals is generally considered to be more accurate (more detail is also provided in *Coles (2001)*) than the delta approach. Hereafter, the confidence interval will be generated via the profile-likelihood approach, unless specified otherwise.

Prior to calculating any return levels, or annual exceedance probability (AEP), it is first important to assess how well the GEV distribution fits the data. As described in Volume 3 — Extreme Wind, there are a number of diagnostic plots and statistical approaches that could be used. Diagnostic plots for the GEV distribution fitted to the annual maximum temperatures are shown in *Figure 5*.

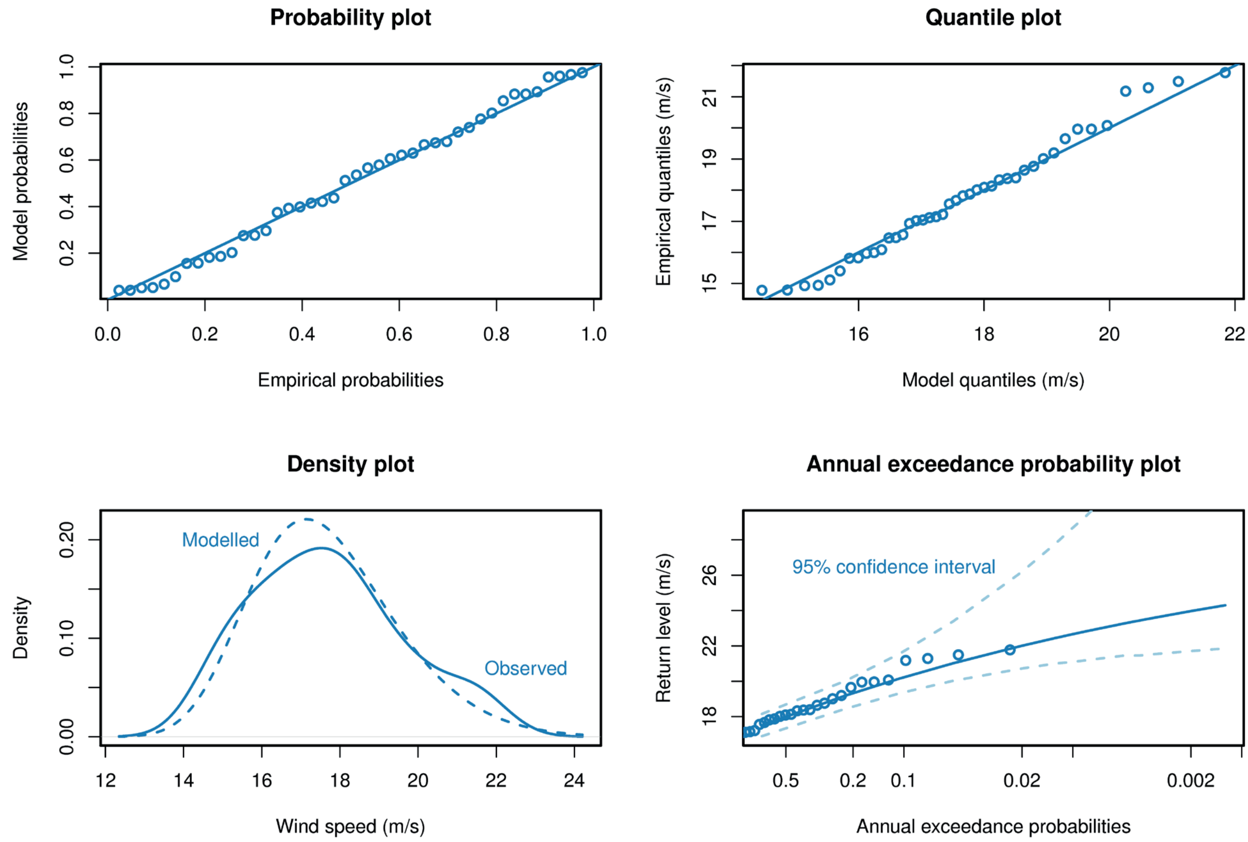

Figure 5. Standard diagnostic plots of the fit of the GEV distribution to the annual maximum daily mean wind speed for Kirkwall.

The probability and quantile plots (top left and top right) help to assess how well the GEV distribution fits the data. A perfect fit would result in a match of the probabilities (or quantiles) of the statistical model to the observed (empirical) probabilities (or quantiles), i.e. all the points would lie on the 1:1 (diagonal) line in each plot. For the annual maximum wind speed data, the probabilities and the quantiles lie close to this 1:1 line, suggesting that the GEV distribution is a reasonable representation of the annual extreme values.

The quantile plot (top right) suggests that the quantiles from the GEV model may underestimate the observed data above 20 m/s. However, some slight deviation of the empirical quantiles from the 1:1 correspondence line is not unusual for the highest quantiles, as shown here, and can occur due to sampling error. Sampling errors occur because a sample of values is observed, rather than the entire population; they are not due to imperfect selection, bias in response or estimation, errors of observation and recording, etc.

The density plot (bottom left chart within *Figure 5* — also known as a probability density plot) compares the empirical probability density derived from the data to the probability density derived from the GEV distribution, with the parameters for location, scale and shape of *Table 3*. Both the empirical and GEV curves are in relatively good agreement with each other, suggesting that the GEV is a reasonable model for extreme annual wind speeds. The 'bulge' in the observed curve for wind speeds greater than 22 m/s could be due to sampling error, or could suggest that there is a physical process not considered in the fitted GEV model and associated with the most extreme annual wind speed events. A tally of the annual maximum data shows that there are only four values greater than 21 m/s, and no values greater than 22 m/s. This suggests that the 'bulge' is more likely to be attributable to sampling error.

Overall, the diagnostic plots for the GEV model suggest that the GEV is a good fit to the annual extreme wind speed. This lends confidence to using the fitted GEV model to calculate AEPs for return levels.

Calculating return levels

Table 4 lists return levels for a number of AEPs. The smaller the exceedance probability, the greater the uncertainty about the return level, a behaviour also noticeable in the annual exceedance plot (*Figure 5* — bottom right) where the 95% confidence interval around the extreme annual wind speed event (return level) widens as the AEP decreases (return period increases). Therefore, caution is urged when using very small AEPs, particularly when the return period extends appreciably beyond the length of the time series used to fit the GEV distribution.

The upper limit for the 95% confidence interval for the AEP of 0.01 and 0.05 is found to be greater than 26 m/s, the current maximum mean daily wind speed observed in the UK for sites at altitudes of less than 100 m. This high upper confidence limit could be a result of the very small number (42 values) of extreme wind speeds available for Kirkwall.

This analysis is illustrative of a particular EVA technique; there are some limitations associated with using only the annual maximum mean wind speeds (block maxima approach), e.g. other extreme values in the same year are ignored. Using a threshold exceedance model, which could potentially use more of the data, may help to overcome these limitations and could result in a more robust confidence interval that may have a lower value for the upper 95% confidence limit of the AEP of 0.01.

Table 4. Return levels for a selection of AEPs along with associated 95% confidence intervals for extreme wind speeds at Kirkwall, calculated from the fitted GEV distribution.

AEP	Mean wind speed	95% confidence intervals
0.5 (1 in 2-year return period)	17.5 m/s	[16.9 m/s, 18.1 m/s]
0.05 (1 in 20-year return period)	22.1 m/s	[20.8 m/s, 26.7 m/s]
0.01 (1 in 100-year return period)	22.8 m/s	[21.2 m/s, 29.5 m/s]

Impact of climate change

The above analysis assumes that wind speeds are stationary, i.e. that climate change will not affect the frequency or the magnitude of these extreme events. However, recent advances in climate modelling have indicated that there could be a small but significant increase in the number of wind storms affecting the UK when analysing model outcomes for 2070 to 2099 (*Zappa et al., 2013*) and that the frequency and intensity of these wind storms could increase during the winter months (*Zappa et al., 2013*; *Mizuta, 2012*). The UK Climate Projections 2009 (UKCP09) project shows plausible changes in the 21st century climate for the UK. These projections state that the spread of possible changes in mean wind speeds across Scotland for the 2050s is strongly influenced by natural climate variability (*Sexton and Murphy, 2010*). According to UKCP09, any projected changes to average wind speeds were found to be much smaller than the variability of winds from year to year (i.e. any potential climate change 'signal' in average wind speed would be swamped by the year-to-year ***noise*** in average wind speed). Therefore, it is currently difficult to state if there are significant shifts in the mean wind speed.

2.1.2 Tornadoes

Definition

The definition of a tornado is 'a rapidly rotating column of air that reaches between the base of a storm cloud and the Earth's surface' (*Met Office, 2018a*). When a funnel cloud reaches the Earth's surface over water, the resulting phenomenon is known as a waterspout (from this point onwards, unless explicitly distinguished in the text, the term tornado will refer to both tornadoes and waterspouts).

Although no tornadoes have been observed at Dounreay in the recent past, there have been instances of tornadoes – or the beginnings of tornadoes (funnel clouds) – occurring in Scotland. It is more common for funnel clouds to be observed and mistaken for tornadoes, especially when seen at a distance, because it is difficult to ascertain whether they reach the surface.

Most tornadoes occurring in the UK occur in England (78%) with only a 2% maximum probability of a tornado occurring within 10 km of any particular point in Scotland, according to *Mulder and Schultz (2015)*. The majority of the literature suggest that tornadoes are most likely to occur during summer and autumn (*Meaden, 1985*; *Holden and Wright, 2004*; *Kirk, 2007*; *Kirk, 2014*; *Mulder and Schultz, 2015*). Although rarer, it is possible for tornadoes to occur in winter (see below).

Instances of tornadoes occurring in Scotland in the recent past include:

- one tornado was reported in Perth on 26th July 2003, although whether it caused any damage was not reported (*BBC, 2003*);
- funnel clouds were observed:
  — near Stonehaven in Aberdeenshire on 25th June 2013 (*The Scotsman, 2013*),
  — near Aberdeen on 24th April 2016 (*Evening Express, 2016*), and 24th August 2017 (*Evening Express, 2017a*),
  — near Inverurie on 4th August 2017 (*Evening Express, 2017b*);
- two waterspouts were observed off the coast of Fife in the Firth of Forth on 6th January 2010 (*BBC, 2010*).

There was no organised study of tornadoes in the UK prior to the founding of the Tornado and Storm Research Organisation (also known as TORRO) in 1974 (see Volume 3 — Extreme Wind). The Tornado and Storm Research Organisation relies on volunteers to collect and collate observations of tornadoes. It also undertakes site investigations to verify tornado reports and measure damage using the tornado intensity scale (*Mulder and Schultz, 2015*). As the data collection is dependent on the number of visible accounts made by volunteers, it is likely that observations are biased towards more populated areas, such as the south-east of England. A degree of over-reporting of tornadoes is also expected due to the presence of funnel clouds being mistaken for tornadoes, despite not actually touching down at the surface or causing damage.

In addition to the likely lack of observers, tornadoes in or near Dounreay could potentially also go unnoticed because there is less infrastructure and tornadoes are therefore less likely to cause damage and be reported. Similarly, if tornadoes manifest at sea as waterspouts, they will only be recorded if they are observed, as they leave no trace. This makes it likely that waterspouts may only be seen in the daytime or could be obscured by other weather phenomena (e.g. low cloud, very intense rainfall or hail).

Data

The Tornado and Storm Research Organisation has updated a map of tornado counts originally produced by *Meaden (1985)*. The map shows tornado counts from 1950 to 2010 for the whole of the UK and makes the following assumptions:

- within each 25 km x 25 km grid square, only tornadoes or waterspouts which made landfall are included;
- if the path of a tornado crossed the border of a grid square, it is counted within each grid square.

In addition to the counts and distribution of tornadoes, the Tornado and Storm Research Organisation also offers information on the intensities and seasonal occurrence of tornadoes.

The tornado count is also adjusted to take into account the fact that 25 years of observations occurred before the formation of the Tornado and Storm Research Organisation in 1974, and data prior to 1974 could be biased by under-reporting as the organisation did not exist to verify observations. The UK saw an average of 30 tornadoes per year from 1950 to 2010, but an average of 36.5 tornadoes per year from 1981 to 2010 (*Kirk, 2014*). On the assumption that this difference can be assigned to under-reporting, the gridded data pre 1974 are adjusted by a factor of 1.22 (= 36.5/30.0). These values were also scaled to represent a 50-year equivalent, that is multiplied by 0.83 (= 50 years/60 years), assuming that tornadoes occur at a constant rate in time. The resulting estimated gridded counts of tornadoes for the 50-year period are shown in *Figure 6*.

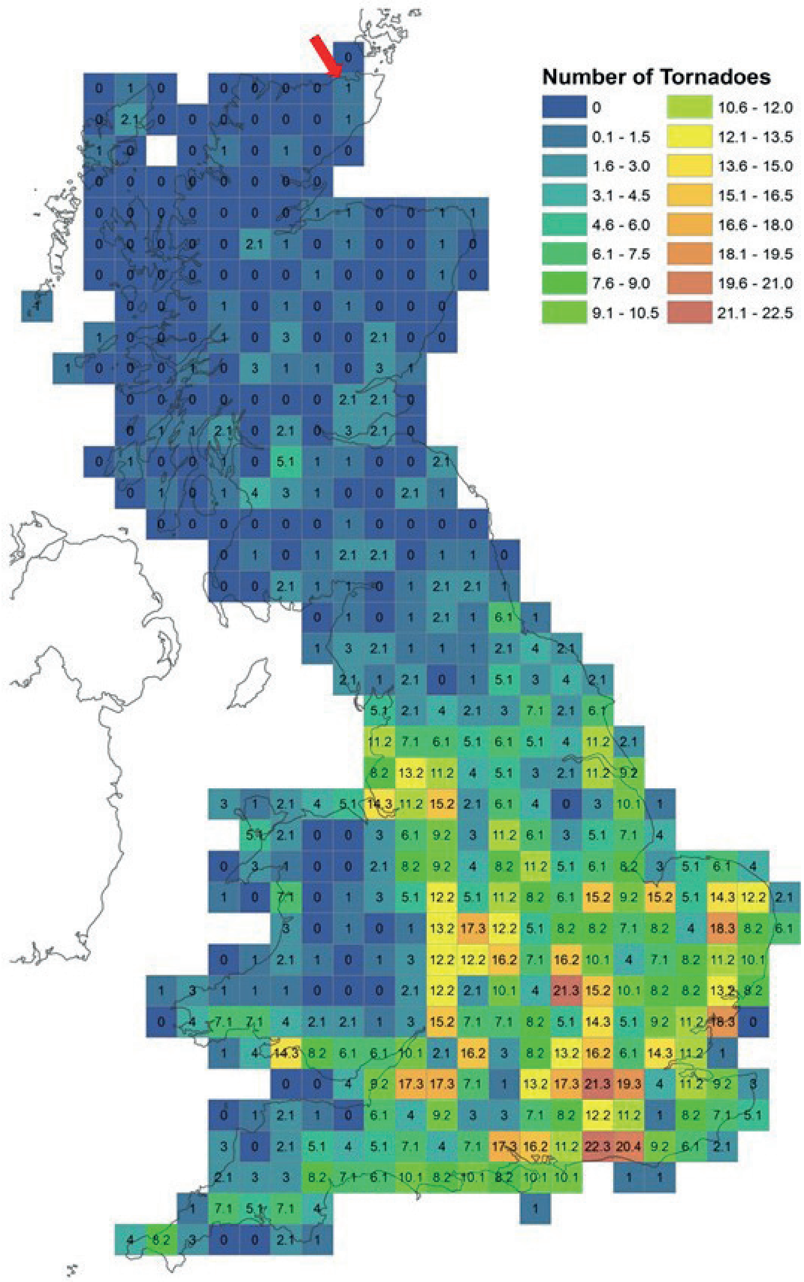

Figure 6. Estimated number of tornadoes per 25 km x 25 km grid square per 50-year period, using data from the Tornado and Storm Research Organisation. The location of Dounreay is indicated by the red arrow. (© Terence Meaden – Tornado and Storm Research Organisation)

Figure 6 highlights the relatively low occurrence of tornadoes across Scotland. The Dounreay area (grid square) has seen one tornado (or waterspout) in 50 years. This low count near Dounreay or in Scotland in general is influenced by a number of factors such as:

Natural spatial distribution of tornadoes

There are on average 34.3 tornadoes per year across the UK (*Mulder and Schultz, 2015*). This corresponds to an average of 4.4 tornadoes per grid square over a 50-year period which is calculated as: 34.3/244,820 km^2 (land area of the UK) x 625 km^2 (area of grid square) x 50 years. However, the distribution of tornadoes is heavily weighted towards the south of the UK where the atmospheric instability is greater during the warm season, where sea surface temperatures are highest (*Holley et al., 2014*), and where higher population densities are present (*Mulder and Schultz, 2015*). According to *Mulder and Schultz (2015)*, the maximum annual cumulative probability of a tornado occurring within 10 km of a specific point in Scotland is 2%, compared to up to 6% between London and Reading.

Under-reporting and under-observing of tornadoes

As previously mentioned, areas with a lower population density are at greater risk of under-reporting tornadoes. This is the case for Scotland and is further emphasised by the fact that Scotland also has less infrastructure (i.e. a tornado would be less likely to cause significant damage).

Terrain and land-use characteristics

Tornadoes can technically develop over any type of terrain but there is evidence to suggest that their development is generally inhibited by very rugged terrain, as seen in cities like London (*Elsom and Meaden, 1982*). Certain land forms such as hills can act as barriers which then create eddies (or vortices) in air flow that can be picked up by passing thunderstorms. Given that Dounreay is generally surrounded by largely flat topography and that the most prevalent direction of travel for tornadoes in the UK is from the south-west (*Meaden, 1985*), terrain in the south-westerly direction of Dounreay would be most likely to propagate tornadoes in this way. Although there are some low-lying hills ~30 km to the south-west of Dounreay, the recorded tornado count is too low to demonstrate effectively that this hilly terrain is disrupting tornado formation.

Coastal effects

Kirk (2007) and *Kirk (2014)* suggested that there were on average approximately three times more tornadoes over land than over sea in the UK. Offshore infrastructure at Dounreay is therefore less susceptible to tornado damage. However, this ratio was found to vary significantly from year to year (*Kirk, 2007*), suggesting that it needs further verification.

Intensity of tornadoes

Tornadoes are categorised by their intensity (see Volume 3 — Extreme Wind). Cumulatively, approximately 95% of UK tornadoes between 1980 and 2012 were between T0 and T3 on the Tornado and Storm Research Organisation scale, and only 5% were T4 or T5 (*Mulder and Schultz, 2015*). Given the average of 34.3 tornadoes per year, this is equivalent to an average of 1.7 tornadoes of strength T4 or T5 per year across the whole of the UK.

Seasonality in tornadoes

Across the UK, tornadoes generally tend to occur during summer and autumn (31.4% and 31.8% respectively) and to peak during late summer, excluding the 1981 outbreak (*Mulder and Schultz, 2015*). The 1981 outbreak occurred when a cold front swept across the UK producing 58 definite tornadoes and 32 probable tornadoes (*Apsley et al., 2016*).

Analysis

The following analysis first characterises the probability of a tornado affecting any location in the UK, then calculates the probability of a T3 to T5 tornado affecting the Dounreay site specifically. To calculate the likelihood of a tornado affecting a location, Dounreay or otherwise, the frequency of occurrence and intensity of the tornado (defined by the damage area), as well as the size of the site, must be taken into account. The intensity, track length, width and area of tornadoes are provided in *Table 5*, based on 767 tornadoes observed from 1980 to 2010 in the UK (*Kirk, 2014*).

Table 5. Tornado wind speed, track length, width and area associated with various tornado intensities in the UK for the period 1981 to 2010. The percentage occurrence of tornadoes of given intensities are collated from 767 tornadoes which occurred from 1981 to 2010. Data in columns 1 to 6 are taken from Kirk (2014); © Royal Meteorological Society 2014. The area of the UK affected by tornadoes every year is calculated by multiplying the track length by the track width by the occurrence.

Intensity	Wind speed (m/s)	Track length (km)	Track width (m)	Track area (km^2)	% occurrence	Area of UK affected every year (m^2)
T0	17 to 24	≤ 0.215	≤ 2.1	≤ 0.000464	8.2	1270
T1	25 to 32	0.22 to 0.46	2.2 to 4.6	0.000465 to 0.00215	26.2	10,000
T2	33 to 41	0.47 to 0.99	4.7 to 9.9	0.00216 to 0.00999	38.2	148,000
T3	42 to 51	1.0 to 2.1	10 to 21	0.01 to 0.046	21.4	176,000
T4	52 to 61	2.2 to 4.6	22 to 46	0.047 to 0.21	5.1	200,000
T5	62 to 72	4.7 to 9.9	47 to 99	0.22 to 0.99	0.8	15,000
T6	73 to 83	10 to 21	100 to 215	1.0 to 4.6	0.1	8000
T7	84 to 95	22 to 46	216 to 464	4.7 to 21	0	0
T8	96 to 107	47 to 99	465 to 999	22 to 99	0	0
T9	108 to 120	100 to 215	1000 to 2100	100 to 464	0	0
T10	121 to 134	216 to 464	2200 to 4600	≥ 465	0	0

First approximation of tornado return periods for the UK

An initial estimate of the probability of anywhere in the UK being affected by T0 to T3 and T4 to T6 tornadoes is outlined in the following calculation. This assumes that tornadoes in the UK are uniformly distributed and the total area of the UK is 244,820 km^2. The area of the UK affected by tornadoes of a given intensity is taken from *Table 5*.

The AEP of any location being affected by a tornado of intensity T0 to T3 is

$$AEP = \frac{0.34\ km^2 \text{ (area of UK affected every year by tornadoes T0 to T3)}}{244{,}820\ km^2} = \frac{1}{720{,}100} \sim 0.000001$$

The AEP of any location being affected by a tornado of intensity T4 to T6 is

$$AEP = \frac{0.22\ km^2 \text{ (area of UK affected every year by tornadoes T4 to T6)}}{244{,}820\ km^2} = \frac{1}{1{,}113{,}000} \sim 0.0000009$$

Tornado return period estimation for the Dounreay site

To determine the return periods of tornadoes at Dounreay, the ratio between the site area and the tornado damage area should be considered. It is apparent from *Table 5* that the damage area of a tornado only exceeds the Dounreay onshore site area (0.54 km^2) at intensities greater than T4. Given that the majority of tornadoes experienced in the UK are T0 to T3, the Dounreay site area is likely to be larger than the tornado damage area. Therefore, in this example, the tornado is treated as a point entity compared to the Dounreay site area.

The counts of tornadoes from *Figure 6* were combined with the percentage occurrence (column 6 from *Table 5*) to estimate the return periods of tornadoes of specific intensities at the Dounreay site.

The annual return level of a tornado can be calculated using a Poisson point process with rate λ (i.e. the number of tornadoes occurring over a specified period) which assumes that:

- tornadoes occur independently and uniformly throughout the area of interest (25 km x 25 km grid square);
- tornado occurrence is stationary with respect to time, i.e. the expected number of tornadoes is the same on an annual basis;
- each tornado is considered a point entity with no allowance made for damage areas.

By weighting the percentage of the grid square affected by the count of tornadoes in a 50-year period, the return levels of a tornado occurring in an area the size of Dounreay can be calculated (assuming spatial homogeneity across the grid square) as:

$$\lambda_S = \lambda_A \times S/A$$

with:

λ_S = Poisson rate, i.e. the probability of a tornado occurring in the specified area in 50 years;

λ_A = number of tornadoes in 50-year period (in this case, 1);

S = site area (in this case, the Dounreay site is 0.54 km^2);

A = 625 km^2 (i.e. area of 25 km x 25 km grid square containing the area of interest).

Using these components, probabilities and return levels of any tornado impacting the Dounreay site are displayed in *Table 6*.

Table 6. Estimated return periods for a tornado and at specific tornado intensities at Dounreay, all rounded to the nearest thousand.

S (km^2)	λ_S	Return period			
		All tornadoes (years)	≥ T3 (years)	≥ T4 (years)	≥ T5 (years)
0.54	0.00086	~60,000	~200,000	~1,000,000	~6,500,000

From the analysis in this case study, there is evidence to show that an extreme wind speed (1 in 100-year event) is equivalent to the wind speed experienced in a T0 tornado, the return period of which is a lot lower (*Table 4*). However, daily mean wind speeds cannot strictly be compared to tornado wind speeds, as these are transient and rotating and therefore exert stronger forces in a matter of several seconds at any one place. For instance, it is not accurate to suggest that a T1 tornado would cause the same damage as a Force 10 wind (Beaufort scale = ~24 to 28 m/s).

Impact of climate change

There is no evidence to suggest that the number of severe tornadoes has changed over the duration of the observational record from 1950 to the present day (as of publication in 2018). In addition, the uncertainties associated with the observations of tornadoes mean that it is not possible to establish any effect of climate change on tornado frequency or intensity over the observational period.

2.1.3 Minor hazards associated with extreme wind speed

Sandstorms

Sand and dust storms are common meteorological hazards in arid and semi-arid regions in other parts of the world. They are usually caused by thunderstorms — or strong pressure gradients associated with cyclones — which increase wind speed over a wide area (*WMO, 2018*). The clouds of particulate matters (e.g. dust, sand) that are whipped up by strong winds can reach very high altitudes in the atmosphere and be transported worldwide. For airborne dust and sand to reach the UK, there needs to be:

- a source of dust (commonly the Sahara Desert); and
- the right weather circulation pattern to transport dust towards the UK (normally a southerly air flow).

The UK normally witnesses this phenomenon several times a year; however, it rarely causes anything more noticeable than a vivid sunset or dust deposits on cars known as 'blood-rain'. Dounreay's geographic location means that it is in the area that is least likely to be affected by particulate matter arriving from a southerly direction. Volcanic ash is another potential source of particulate matter — please refer to Volume 7 — Seismic, Volcanic and Geological Hazards, and Case Study 1 — Trawsfynydd for further detail.

Quantifying the effect of Saharan dust on the Earth's climate system is challenging (*Rocha-Lima et al., 2018*), and understanding the impacts of residual Saharan sand at a much smaller scale on the energy infrastructure at the Dounreay site is not possible without reliable observation records.

Future changes in sand and dust storms are very dependent on climate change scenarios for precipitation, winds and temperature, as these could affect the way in which dust is transported from a source region. Changes will also be dependent on future land use (e.g. vegetation degradation) as this could affect the availability of dust in a source region. With a lack of reliable observation data it is not possible to comment on future changes for the Dounreay site.

2.2 Extreme precipitation

This section covers the analysis of extreme rainfall using extreme value theory, the impact of climate change and a brief analysis of extreme snow and humidity.

2.2.1 Definition

The definition of an extreme rainfall event for the energy sector and of any associated rainfall threshold will differ depending on the vulnerability and exposure of the asset. For example, the nuclear industry has to understand the response of drainage systems to extreme rainfall events for flood risk assessments.

The characteristics of extreme rainfall events are defined by their intensity, duration and spatial distribution (see Volume 4 — Extreme Precipitation). The impacts of extreme rainfall can affect a broad range of energy infrastructure both onshore and offshore. In relation to Dounreay, examples are outlined briefly below.

According to SEPA's flood outline (*SEPA, 2018*):

- There are areas in the vicinity exposed to a medium to high likelihood of surface water (pluvial) flooding. Surface water flooding, often caused by high intensity summer rainfall (and also low intensity winter rainfall), overwhelms drainage systems and can particularly affect urban areas. This can lead to the flooding of power stations and transformers, and also affect roads leading to the site, preventing safe access by key personnel and impacting on the ongoing operability of an asset.
- In Lower Dounreay and to the southwest there is a medium to high risk of river (fluvial) flooding. Substations and pumping stations are at a greater risk of river flooding.
- There is no groundwater flooding in this area.

An example of an impact on the offshore wind sector is erosion of the wind turbine blade leading edge. The impact fatigue caused by collision with rain droplets, hailstones and other airborne particles is a severe problem for wind turbine blades; extreme rainfall events reduce their service life (*Bech et al., 2018*).

Extreme rainfall can directly result in different types of flooding: pluvial (surface water), fluvial (river) and groundwater. In turn, these flooding events can give rise to serious impacts to life and energy infrastructure. They are often outcomes of four main contributory factors (*Collier et al., 2002*):

- intensity of precipitation;
- duration of precipitation;
- the wetness of the ground;
- the response of the rainfall catchment.

Pluvial flooding occurs when natural and man-made drainage systems cannot deal with the volume of rainfall. It is particularly hazardous in urban environments, as sudden and intense rainfall cannot drain away easily (*Pitt, 2008*). River flooding occurs as a result of water overflowing from river channels. Groundwater flooding often persists long after fluvial flooding has subsided (see Volume 4 — Extreme Precipitation) and can be very difficult to address as substantial work may be necessary to conduct flows away to a natural aquifer (*LGA, 2018*). Below a certain depth, if the ground (rock, rock fractures or materials such as gravel, sand or silt) is permeable enough to hold water, it can become saturated. The upper surface of this saturation level is known as the water table and the zone beneath is called an aquifer.

Intensity and duration of precipitation are meteorological contributors, whilst wetness of the ground and response of the rainfall catchment are hydrological. This case study concentrates on the meteorological contributors. Depending on the chosen definition, an extreme rainfall event may span multiple days. The term 'wet spell' is commonly used to describe 'a period of a number of consecutive days in which precipitation exceeding a specific minimum amount has occurred' (*WMO, 1966*).

When characterising extreme rainfall for energy infrastructure, the characterisation method will depend on the factors of interest outlined above. For example, in this case study, a 24-hour duration has been selected because it is constrained by the available observation data. Disaggregation techniques are available to convert daily rainfall to hourly, but this has not been performed in this illustrative analysis.

2.2.2 Data

By convention, all meteorological weather stations record daily rainfall as a total over the period 09:00 GMT to 09:00 GMT the following day. Total daily rainfall is therefore used in the EVA analysis applied to rainfall.

The top ten daily rainfall totals for weather stations closest to Dounreay are shown in *Table 7*. As Dounreay's rainfall record was not sufficiently long, Wick Airport was identified as the most suitable alternative weather station to Dounreay, from all the weather stations described in *Table 2* (i.e. it is the station with the smallest mean squared deviation as per the approach described in *Appendix A.2*).

Table 7. Top ten rainiest days for weather stations closest to Dounreay. (© Crown Copyright Met Office 2018)

Rank	Top 10 rainiest days at Dounreay		Top 10 rainiest days at Kirkwall		Top 10 rainiest days at Wick Airport		Top 10 rainiest days at Stornoway Airport	
	Date	Daily rainfall (mm)	Date	Daily rainfall (mm)	Date	Daily rainfall (mm)	Date	Daily rainfall (mm)
1	17th Aug 1964	62.5	4th Oct 1979	54.9	6th Jun 2017	59.4	27th Aug 1933	69.8
2	8th Sep 1965	50.8	17th Dec 1984	53	17th Aug 1964	54.9	19th Jan 1989	64.7
3	4th Aug 1962	45.7	2nd Nov 2013	50.2	3rd Sep 2009	52.4	30th Oct 1989	64
4	16th Aug 1970	35.6	19th Oct 2013	49.9	8th Sep 1976	49.7	23rd Aug 1957	57.5
5	21st Jul 1965	34.8	31st Oct 1970	47.8	27th Aug 2011	46.2	6th Aug 2007	54.8
6	3rd Sep 1963	34	6th Jun 2017	44.6	2nd Nov 2013	42.4	5th Aug 1982	52.8
7	26th Jun 1963	33	26th Oct 2006	44.2	16th Aug 1970	41.4	18th Jan 1959	52.2
8	19th Nov 1980	32.8	8th Sep 1965	43.8	4th Oct 1979	41.2	4th Sep 1936	49.2
9	31st Jan 1983	32.7	27th Aug 2011	43.8	17th Dec 1984	38.4	4th Jun 1937	46.1
10	1st Sep 1966	32	3rd Aug 1962	43.7	1st Nov 2009	38.2	22nd Sep 1945	45.9

Stornoway – located on the Isle of Lewis, to the west of the Scottish mainland – experienced the largest 24-hour rainfall of 69.8 mm compared to the other weather stations listed in *Table 7*. This is probably due to its location as the Isle of Lewis is fully exposed to Atlantic depressions that approach from the west and associated frontal rainfall which may be increased with orographic lift, i.e. the forcible uplift of air by terrain which creates clouds and rainfall (see Volume 4 — Extreme Precipitation). The Kirkwall weather station is located on Orkney and, like Stornoway, is more exposed to Atlantic depressions. Dounreay and Wick are located at coastal sites on mainland Scotland. Dounreay is on the north coast of Caithness and Wick on the east coast of Caithness. Both weather stations experience similar top ten largest 24-hour rainfall totals and also similar months of occurrence, because they both experience similar rainfall mechanisms due to the flat terrain and lying in the lee (rain shadow) of higher ground.

2.2.3 Analysis

In this illustrative EVA, a point-process generalised Pareto distribution (PP-GPD) that allows for the estimation of both the frequency and magnitude beyond which a threshold, is exceeded, is used to model extreme daily rainfall events using rainfall data from Wick Airport. An initial analysis of the fit to the daily rainfall totals is presented here. The limitations of this initial analysis are highlighted, and results from a more advanced analysis which seeks to improve the model fit by including a covariate for the *North Atlantic Oscillation* (NAO) are discussed. *Appendix A.3* provides more details and also contains a discussion of further considerations that should be taken into account.

Selecting extreme rainfall events

Unlike the block maxima approach, the threshold approach considers all observations beyond a prescribed threshold, including potentially informative but less extreme events.

Several methodologies exist that help the user to choose a suitable threshold. In this case study, a range of daily rainfall thresholds between 15 mm and 50 mm were initially considered using all available daily rainfall data from Wick Airport. Ideally a threshold should be low enough so that a sufficient number of observations are classified as extreme in order to allow a PP-GPD to be fitted. Volume 3 — Extreme Wind and Volume 4 — Extreme Precipitation provide further discussion on the importance of threshold choice in relation to the number of extreme events. For each potential threshold, a PP-GPD model was fitted and the parameters of the PP-GPD noted alongside the number of rainfall events classified as extreme. From the potential candidates, a threshold was chosen where the values of the parameters for PP-GPD across different thresholds seemed relatively stable and a suitably large number of events were selected. For daily rainfall at Wick Airport, a threshold of 20 mm was chosen and resulted in 119 events classified as extreme rainfall events.

An assumption that is usually made prior to the fitting of a PP-GPD is that the extreme events are independent of one another. For Wick Airport, the large majority (over 90%) of the extreme rainfall events were separated by more than 10 days and it was assumed in the analysis that the extreme rainfall events were indeed independent.

Fitting a PP-GPD model

The diagnostic plots of the fit of the PP-GPD using a threshold of 20 mm are shown in *Figure 7*. Any appreciable deviation from the 1:1 line in the probability and quantile plots could indicate that the fitted extreme value distribution may not represent the observed data well. The concave nature of the probability plot here suggests that the model broadly underestimates extreme rainfall data, a result also observed in the density plot. The quantile plot magnifies any differences between the tails of the fitted and observed distributions. In this case, there appears to be some deviation between the observed and fitted model in the tails, with the suggestion that the model underestimates the most extreme rainfall totals. The density plot further highlights the mismatch between the observed distribution and that of the fitted PP-GPD model for the most extreme rainfall events. In the AEP plot, there is a suggestion that for the larger probabilities the observed extreme values fall outside of the 95% confidence interval for the fitted PP-GPD model.

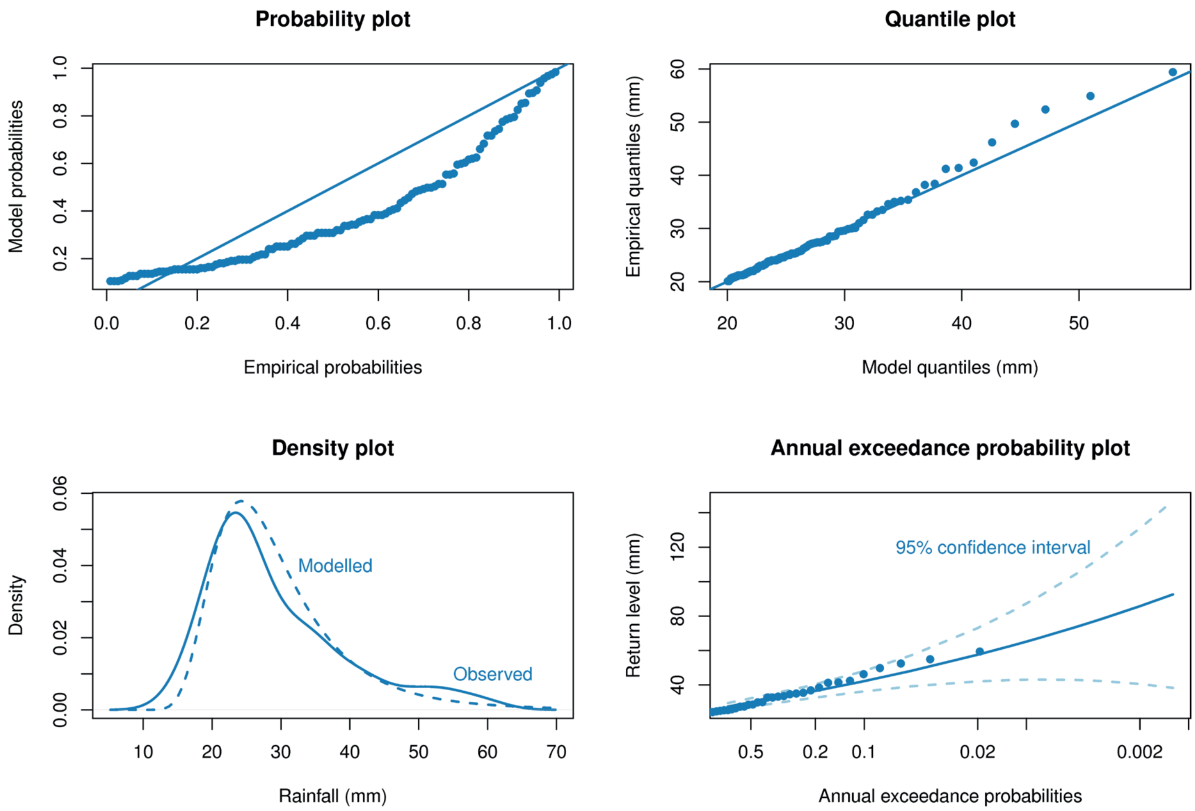

Figure 7. Diagnostic plots of the fit of the PP-GPD distribution to the extreme rainfall at Wick Airport. The confidence intervals are approximate 95% normal confidence intervals.

The diagnostic plots therefore suggest that the current PP-GPD model does not provide a particularly good fit to the data. As a result, the use of any return levels generated from this model to provide guidance on the nature of expected extreme rainfall events would be highly questionable, and confidence in the accuracy of these return levels would be low.

As a result, it is necessary to investigate some alternative PP-GPD models. One possible model is a PP-GPD model with the NAO as a covariate, as in the positive phase of the NAO the probability of extreme rainfall is reduced from spring to autumn and increased in the winter (*Brown, 2017*). The diagnostic plots and formal statistical tests (see *Appendix A.3.1*) show that including the NAO as a covariate leads to a much improved fit of the PP-GPD model to the rainfall extreme events. The return levels from this analysis are shown below to illustrate the output of such an approach.

Calculating return levels

For a given value of the NAO index, it is possible to derive NAO-specific AEPs and return levels – known as effective return levels at they depend on the value of the NAO. *Table 8* shows effective return levels for AEPs of 0.5, 0.05 and 0.01 conditioned on standardised values of the NAO index, along with the associated 95% confidence intervals. The largest rainfall totals generally occur when the NAO index is large and negative, which is broadly in agreement with the results from *Brown (2017)*.

However, care should be taken with the interpretation of the rainfall return levels in this table, as they are now for specific values of the NAO index and calculated assuming that the specific NAO index is fixed at a constant value for each day of the year, which is not the case. For example, the daily rainfall total has a 50% chance of being greater than 32 mm in a single year only if the NAO index is –3 for all days in that year.

Table 8. Daily rainfall total effective return levels (mm) associated with particular AEPs, along with 95% confidence intervals (calculated using the delta approach) given particular values of the NAO index.

		Standardised NAO index						
		–3	–2	–1	0	1	2	4
AEP	0.5	32 (27, 36)	30 (27, 34)	29 (26, 31)	27 (25, 29)	26 (24, 28)	24 (21, 27)	23 (19, 27)
	0.05	52 (43, 62)	51 (42, 60)	49 (41, 58)	48 (39, 57)	46 (37, 55)	45 (36, 54)	43 (34, 53)
	0.01	70 (48, 90)	68 (46, 89)	66 (45, 87)	65 (43, 86)	63 (41, 87)	62 (40, 83)	60 (38, 82)

Instead of deriving the return levels given values of the NAO index and AEPs as shown in *Table 8*, a more realistic approach would be to take the average of the effective return levels for each observation of the NAO index. An example of such an approach is given in the analysis of extreme air temperature provided in Case Study 1 — Trawsfynydd and as such is omitted here for expediency.

It may be possible to improve this PP-GPD model further, by revisiting the assumption that the extreme events are independent of one another. Failure to take into account dependency between extreme events can lead to confidence intervals that are too small, and actions taken based upon these results run the risk of underestimating the true range of any return levels associated with an AEP. The details of an approach which adjusts the analysis to ensure that the extreme events are independent are provided in *Appendix A.3.2*.

2.2.4 Impact of climate change

The impact of climate change on rainfall extremes is an area of active research, particularly in the context of short-term extreme rainfall events which typically arise from convective storms. *IPCC (2013)* reports that globally it is very likely over most mid-latitude land masses that there will be an increase in the frequency, intensity and amounts of heavy precipitation by the end of the late 21st century (2081 to 2100). By the 2080s, the high emissions scenario projections of future northern Scotland climate change from UKCP09 broadly indicate that winters are projected to become wetter and summers are projected to become drier. However, for summer projections this is only a part of the whole story, as small-scale, convective rainfall is not well represented in the climate models underlying UKCP09. Climate modelling and the level of scientific understanding has improved since UKCP09; very high-resolution climate simulations over the UK, which can model convective storms and clouds at a smaller scale than traditional climate models, are now being run. Initially this has been carried out for the southern half of the UK (*Kendon et al., 2014*) and has been recently updated to generate high-resolution projected changes in rainfall over Scotland and northern England (*Chan et al., 2018*). *Chan et al. (2018)* showed that for Scotland and northern England:

- summer mean rainfall could decrease due to large decreases in the rainfall frequency, but the intensity of extreme rainfall events could increase;
- winter mean rainfall could increase, with increases in the future intensity of extreme rainfall events possible, however not as much as during the summer.

2.2.5 Minor hazards associated with rainfall

Extreme snow depth

Precipitation can fall as snow when the air temperature is below 2 °C. In the UK the heaviest snowfalls tend to occur when the air temperature is between 0 °C and 2 °C. When snow falls through dry, cold air (e.g. a polar continental air mass, see Volume 4 — Extreme Precipitation), the flakes will be small and powdery, and the snow is more likely to drift as the flakes will not stick together. When the air temperature is warmer than 0 °C the flakes will melt around the edges and stick together to become larger heavy flakes known as 'wet snow'. Very cold air masses during the winter are associated with northerly and easterly winds bringing with them snow to the Dounreay location.

Snowpack is defined as the total snow and ice on the ground, including both new snow and the previous snow and ice that has not melted. Constantly changing weather factors including temperature, snowfall, wind speed and direction can affect the strength and stability of the snowpack.

Extreme snowfall can impact energy sector assets and infrastructure, for example:

- the mass of the snowpack and its effect on the structural integrity of assets, e.g. the roof of a power substation;
- snow drifts can have indirect effects such as disruption to access routes, and can lead to problems restoring power;
- snow melt has the potential to cause flooding, e.g. snow melt leads to excess water amounts and rising water levels that could lead to the flooding of a pumping station.

The National Climate Information Centre (NCIC) records show that overall, for the period 1981 to 2010, Caithness had an annual average of 20 to 30 days of snow lying and 40 to 50 days of sleet/snow falling.

Although snow depth is a measured variable at 09:00 GMT at most meteorological observation stations, the impacts of snow depth and hence snow loads on infrastructure and assets can be found by referring to official guidance documents. For the Dounreay onshore location, guidance is given in the Eurocode BS EN 1991-1-3:2003, *Eurocode 1 — Actions on Structures, Part 1 to 3: General Actions — Snow Loads*. Eurocode 1 provides guidance on the characterisation of snow loads to be used for the structural design of buildings and civil engineering works. For a full description of Eurocode 1 please refer to Volume 4 — Extreme Precipitation.

The National Annex to Eurocode 1 provides a characteristic ground snow load map for the UK and Ireland. The map characterises zones of ground snow load at 100 m above mean sea level by splitting the UK into specific zones. For sites below 100 m altitude, the map value can be used without the altitude modification. For the Dounreay onshore site, the ground snow load (with an annual exceedance probability of 0.02 (1 in 50-year event)) at 100 m is characterised as 0.6 kilonewtons per square metre (kN/m^2).

For the design and operation of offshore structures at Dounreay, snow and ice could have an impact. Snow and ice offshore is not investigated in this case study, but many standards exist for different types of offshore structures. For example:

- DNV-OS-J101 — *Design of Offshore Wind Turbine Structures* — provides guidance on snow and ice accumulation:
  - ice accretion build-up from sea spray, snow and rain and air humidity;
  - snow and ice loads due to snow and ice accumulation;
  - possible increases of cross-sectional areas and changes in surface roughness caused by icing;
  - for buoyant structures, the possibility of uneven distribution of snow and ice accretion.
- DNV-OS-J103 — *Design of Floating Wind Turbine Structures* — provides specific guidance on floating wind structures, but makes extensive reference to DNV-OS-J101.
- ISO 19901-1:2015 — *Petroleum and Natural Gas Industries — Specific Requirements for Offshore Structures — Part 1: Metocean Design and Operating Conditions* — provides guidance on snow and ice accretion.
- HSE — Offshore Technology Report (OTO) 2001/010 *Environmental Considerations* and 2001/013 *Loads* (*HSE, 2002*) — provides guidance on:
  - extreme snow and ice and their interaction with extreme winds;
  - snow and ice environmental loads.

The UKCP09 probabilistic projections of future changes in snow by the 2080s indicates that there could be a reduction of 60% in future heavy snowfall events (measured by changes in the 90th percentile of winter snowfall rate) over Scotland (*Brown et al., 2010*). The UKCP09 projections also showed that by the 2080s during winter there could be a reduction of 70% in the number of days with falling snow in northern Scotland. However, *Brown et al. (2010)* also state that the UKCP09 projections were found to produce unrealistic large uncertainties in future changes, and large biases were found between the historical record and the regional climate model historical period. Therefore, no clear statement can be made on future changes in snow for the Dounreay area.

Humidity

Humidity is used to measure the amount of water vapour in the air. Although there are a number of different definitions that can be used to specify humidity, this case study focuses on relative humidity.

Relative humidity is the most common measure of humidity. It measures how close the air is to being saturated – that is, how much water vapour there is in the air compared to the maximum amount of water vapour the air could theoretically hold at that temperature. The warmer the air, the more water vapour it can hold. If the relative humidity of the air is 100%, then it is fully saturated (*Met Office, 2018b*). In the presence of cloud condensation nuclei, fully saturated air will condense into droplets, forming clouds. It is possible to obtain values of relative humidity greater than 100% when air contains more water vapour than is required to saturate it at its existing temperature — this is called supersaturation. Relative humidity values greater than 100% are rarely seen because they would require the absence of cloud condensation nuclei so that the water vapour does not condense.

Fog is caused when the air near the surface cools to such an extent that water vapour begins to condense forming a suspension of water droplets, i.e. it normally occurs when the relative humidity approaches 100%. By international agreement, fog is defined when it reduces visibility to less than 1 km. However, UK forecasts for the public generally define fog as a reduction in visibility to less than 180 m. Freezing fog forms in the same way as fog; it occurs when temperatures are below 0 °C but the droplets remain as liquid. The liquid needs a surface to freeze upon, and when they come into contact ice crystals form. This is referred to as rime and is a characteristic of freezing fog (see Volume 4 — Extreme Precipitation).

The NCIC records show that overall, for the period 1981 to 2010, Caithness had an annual average relative humidity of 60 to 65%. The highest and lowest recorded daily relative humidity values at Wick are 100% and 50.6% respectively (values based on the period 1968 to 2017).

The measure of relative humidity values greater than 95% is a useful way to indicate air approaching saturation. In Dounreay, 11.9% of the hourly record had relative humidities greater than or equal to 95%, while at Wick this figure was 14.7% (measured over the respective station's record length). These values are similar to those observed for the whole of the UK (15.9%) which were computed relative to the number of observations in the database for that station.

The impacts of fog and humidity on both the onshore and offshore energy infrastructure and operations for the Dounreay site are listed below:

- The primary impact is reduced visibility. This in turn affects safe operations on land and at sea; for example, the disruption of helicopter flight plans to offshore wind farms which follow strict aviation guidelines.

- A specific impact of freezing fog is that it can affect vertical surfaces such as overhead wires, pylons and transmitting masts, by causing a build-up of rime.
- Although not explicitly investigated in this case study, humidity and salt can impact offshore and nearshore infrastructure. Humidity can cause corrosion and condensation, and airborne salts can attract moisture and accelerate corrosion processes. Moisture ingress into internal electrical and mechanical systems of wind turbines can affect long-term operations and costs.

Relative humidity can be indirectly derived from *dry-bulb* and *wet-bulb temperatures*, using psychrometric charts. Both wet-bulb and dry-bulb temperatures are typically measured at Met Office weather stations. For a definition of dry-bulb temperature, see Volume 2 — Extreme High and Low Air Temperature.

To calculate the probabilities of extreme humidity, the wet-bulb temperature can be analysed in a similar way to the way in which dry-bulb temperatures were analysed in Case Study 1 — Trawsfynydd (this method is not demonstrated here). However, it should be noted that it is not appropriate to combine the output from a univariate EVA of dry-bulb temperature with the output from a univariate EVA of wet-bulb temperature. This is because the most extreme dry-bulb temperatures and the most extreme wet-bulb temperatures will not necessarily occur concurrently.

Regarding future changes in extreme humidity, UKCP09 indicates that there is considerable uncertainty associated with the change in relative humidity across the UK, with projected changes in relative humidity under a given scenario often indicating both a decrease and an increase. For example, under a high emission scenario, in winter (summer) the distribution of change ranged from –3% (–24%) for the 10th percentile to +6% (+4%) for the 90th percentile (*Boorman et al., 2010*). For a medium emission scenario, again there is still some considerable uncertainty with the percentage change ranging from –3% (–20%) to +5% (+3%) for summer (winter).

Probabilistic projections of fog were not provided in UKCP09. However, a small ensemble of 11 climate models is available. This ensemble shows considerable uncertainty in the projected changes in numbers of fog days associated with the north coast of the Scottish mainland (*Boorman et al., 2010*).

2.3 Coastal/offshore flooding hazards

In the vicinity of the Dounreay coastal site, flood-related hazards can occur either onshore or offshore. As noted in *Section 1*, onshore coastal flooding is covered in Case Study 2 —

Teesmouth and therefore is not directly mentioned here. This section focuses on flood-related hazards that could occur at offshore infrastructure. Please note that Volume 6 — Coastal Flooding addresses the marine phenomena that can lead to flooding and hence they are referred to as 'flood-related' hazards within this study.

2.3.1 Characterisation of offshore flooding hazards

Some offshore structures are floating, whereas others are fixed onto the sea bed. They are often exposed to strong winds, waves and currents. These can have a profound impact on the loading of the offshore structures. Here, loading is defined as a force exerted on a structure, which the structure should be designed to withstand. Wave loading is usually considered to be the most important of all environmental loadings for an offshore structure. In addition, extreme wave heights could overtop defences and lead to the accumulation of water.

Sea waves can be caused by many factors including: tide-forming forces (of the moon and the sun); winds; fluctuations in atmospheric pressure; underwater earthquakes; deformations of the ocean floor. The main factors affecting wave heights are: wind speed; wind duration; fetch length (distance that wind can travel over open water); depth of water; roughness of the sea bed; direction and speed of the tide. In the offshore environment, compared to coastal:

- the water depth tends to be much greater;
- the wind tends to be much stronger;
- the wave height tends to be much higher.

The forces on a structure are caused by the motion of the water due to the waves and the subsequent loadings are usually much greater than for wind. Wave height and wave period need to be defined and the forces due to wave action need to be calculated accordingly. Usually the maximum wave with a return period of 100 years (i.e. a 0.01 AEP event) is chosen for offshore structure designs, although other return periods, such as 1 in 50 (0.02 AEP), are used for offshore installations (*HSE, 2002*). Therefore, this section focuses on analysing wave height data from wave buoys in the vicinity of Dounreay and assesses the impact that climate change may have.

Additionally, tsunamis present a significant hazard to offshore structures. Tsunamis are waves resulting from any sort of major displacement of water in the ocean such as earthquakes, submarine landslides, volcanic eruptions, or meteorite impacts. Tsunamis are very dangerous as they travel quickly and are difficult to detect. However, tsunamis affecting the British Isles are extremely uncommon; there have only been two confirmed cases in recorded history, one caused by the Storegga slide (approximately 7300 to 7200 years ago), another caused by the Lisbon earthquake of 1755. Meteo-tsunamis (tsunami-like waves of meteorological origin) are somewhat more common, especially on the southern coasts of England around the English and Bristol Channels.

Ice loading is also a primary problem for marine structures (under water) in the arctic and subarctic zones. However, risk from ice is not considered to be a significant issue along the UK shoreline.

Generally, the sea is classified into shallow, deep and ultra-deep areas. The precise meaning of these terms varies globally and over time; one classification of water depths (*Ranakoti, 2003*) is as follows:

- 0 to 350 m deep: shallow water/sea;
- 350 to 1500 m deep: deep water/sea;
- beyond 1500 m deep: ultra-deep water/sea.

The water depth in the offshore area north and north-west of Dounreay between the Faroe Islands, Shetland and Hebrides, is generally around 350 m and thus most offshore structures would be considered as shallow water structures under this classification.

Offshore infrastructure size depends on the facilities that need to be installed on top side, e.g. oil rig, living quarters, helipad, etc. Offshore structures need to be designed by considering a range of types of load, such as:

- permanent (dead) loads (e.g. load of the structure);
- operating (live) loads (e.g. all equipment on the permanent load such as helicopters, ship moorings, etc.);
- environmental loads (e.g. wind, waves, earthquakes).

In addition to wave loads, wave height is also one of the key factors for consideration in offshore structure design to reduce the health and safety risk. For example, due to the damage to offshore structures by Hurricanes Katrina and Rita in 2005, the American Petroleum Institute released a new set of standards for offshore platforms (*Zhang, 2017*). In the 1940s, platforms tended to be 9 to 12 m above sea level (ASL); in the 1990s, this had increased to more than 21 m ASL. Since Katrina and Rita, they have often been above 28 m ASL, which is well above the highest recorded wave height in the Scottish sea (see *Section 2.3.3* and WaveNet for wave statistics in the area). However, wave dynamics and structural design considerations are not part of this study.

2.3.2 Monitoring and forecasting of waves

WaveNet is the strategic wave monitoring network for the UK and is provided by the Centre for Environment, Fisheries and Aquaculture Science (Cefas). It provides a single source of real-time wave data from a network of wave buoys located in areas at risk from flooding. In operation since 2002, WaveNet collects and processes data from the Cefas-operated Datawell Directional Waverider buoys. The WaveNet system also gathers wave data from a variety of third-party platforms and programmes (industry and public sector-funded), all of which are freely available for visualisation on the WaveNet website (*Cefas, 2018*). The WaveNet interactive map shown in *Figure 8* gives a clear picture of the wave conditions along the coastline at a glance. A red arrow indicates wave direction, a blue arrow indicates wind direction, and a number indicates significant wave height.

Further details can be found in Volume 6 — Coastal Flooding regarding monitoring and forecasting of waves.

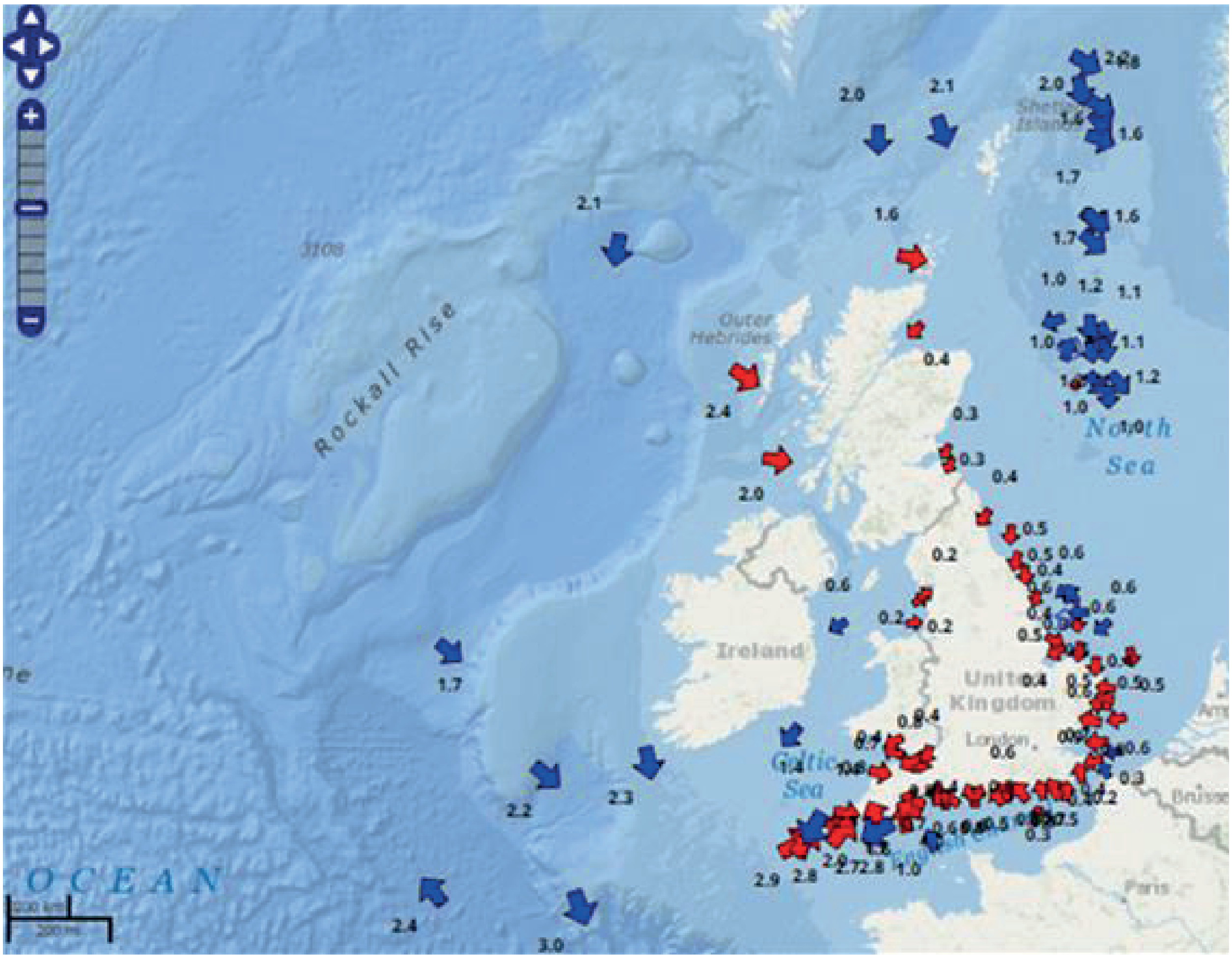

Figure 8. WaveNet map showing significant wave heights as measured by buoys on 27/04/2018 at 14:00hrs. Almost real-time values can be obtained through the live online map. The values on the map are in metres. The map also shows wave direction (red arrows) and wind direction (blue arrows). (Source: Cefas (2018); © Crown Copyright 2018)

2.3.3 Wave statistics near Dounreay

There are a number of wave buoys deployed along the north coast of the Highlands in Scotland; see *Figure 9*. Wave data (graphical views) around Dounreay have been extracted from three current deployments (Billia Croo, K5 buoy, West of Hebrides) and from one historical deployment (at Dounreay; see *Figure 9*) using WaveNet. These stations have been chosen as they are the nearest stations to the site. Billia Croo and West of Hebrides are the two nearest stations that are currently active. The K5 buoy is further from Dounreay, but it is the only station in the general vicinity that is currently active in the deep sea. The historical deployment at Dounreay is closest to the site of interest and, as such, data from these stations will provide the best picture of wave characteristics for Dounreay. However, data are available only for a very short period of three months in 1997 (October for a few days, November and December), and two months in 2001 (April and May). Data from the deployment in Moray Firth, though nearer to Dounreay, have not been used as it is on the east coast and also inside a firth. Availability of wave data at these stations is presented in *Table 9*, while statistics on wave data (minimum, maximum and average) are presented in *Table 10*.

Digital data from West of Hebrides were downloaded from Cefas WaveNet. Digital data from the Billia Croo and K5 buoys are not downloadable; it is only possible to observe maps of the data online and as such the minimum, maximum and average values are not explicitly known for these two stations. It should be noted that Billia Croo is a third-party data monitoring station maintained by EMEC. The maximum values for these two stations (as in *Table 10*) have been estimated as an approximation taken from the wave graphs included in *Appendix B* (*Figures 14* to *17*). A fuller analysis of wave height data (using EVA as in *Sections 2.1* and *2.2* for extreme wind and rain respectively) would require longer data series which could be obtained from hindcast modelled datasets (although it should be noted that extremes extracted from model data can be unreliable).

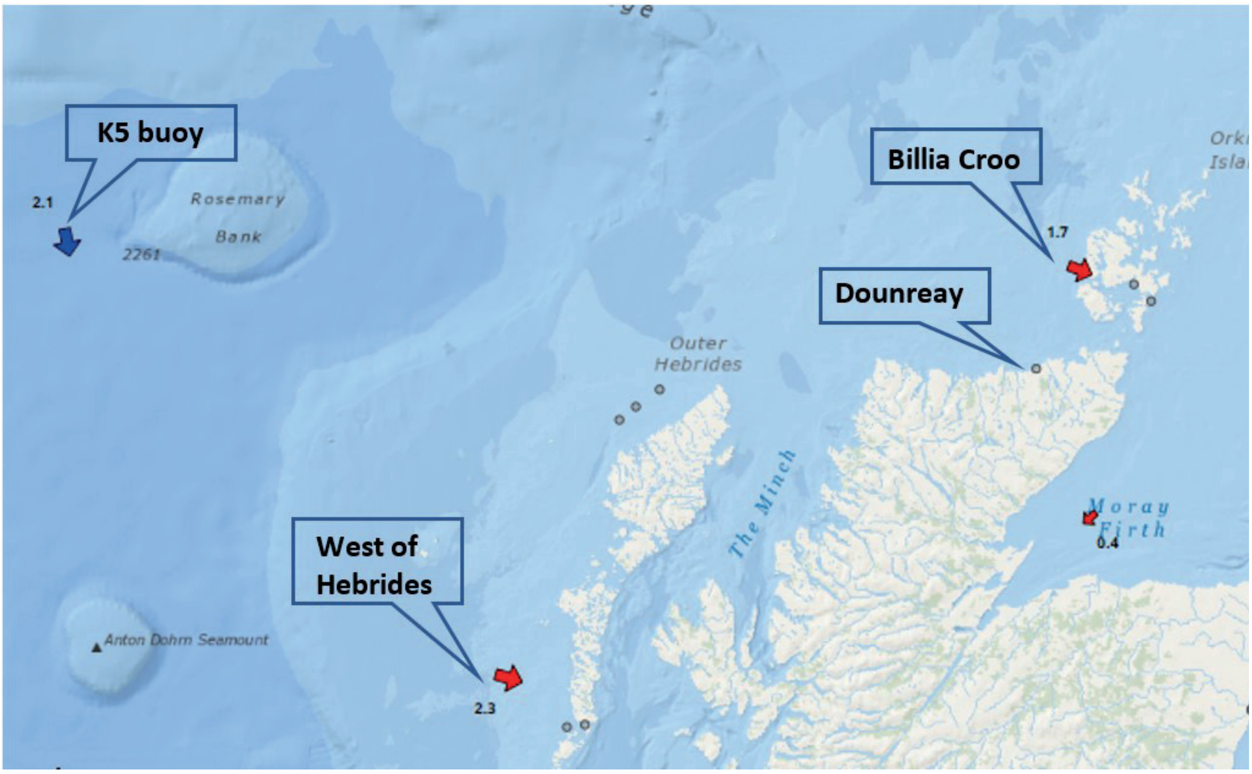

Figure 9. WaveNet map showing the location of current deployments (red and blue arrows) and historical deployments (grey circles) around Dounreay. Significant wave height is reported in metres (numbers on the map), as measured by buoys on 27/04/2018 at 14:00hrs; date and time are almost real time on the live online map, wave direction is indicated by red arrows and wind direction by blue arrows. (Source: Cefas (2018); © Crown Copyright 2018)

Table 9. Wave data availability around Dounreay. (Source: Cefas (2018); © Crown Copyright 2018)

Station name	Deployment status	Data availability
Billia Croo	Current	2015 to 2018
K5 buoy	Current	2007 to 2018
West of Hebrides	Current	2010 to 2018
Dounreay	Historical	1997: Oct, Nov and Dec 2001: April and May

Table 10. Wave data statistics around Dounreay. (Source: Cefas (2018); © Crown Copyright 2018)

Station name	Max depth (m)	Wave height (m)		
		Min	Max	Average
Billia Croo	-	-	>11	-
K5 buoy	-	-	>15	-
West of Hebrides	-	0.29	16.39	3.02
Dounreay	26.4	0.1	4.0	0.94

2.3.4 Climate change consideration

The climate change allowance for wind speed and wave height is presented in *Table 11*. For flood risk assessment at coastal, estuarine and offshore installations, both wind speed and wave height should ideally be analysed in case of a joint event with sea level rise. The percentage increases in wind speed and extreme wave height shown in *Table 11* should be applied in a way that considers the accumulative effect over time. For example, for a 1 in 100-year (1% AEP) event, if the wave height is 4 m at the baseline year of 1990, then the 5% allowance (i.e. 0.2 m) should be added to the 4 m wave height during 1990 and 2055, giving 4.2 m wave height; and subsequently a further 10% allowance (i.e. 0.4 m) should be added to the 4.2 m wave height between 2056 and 2115, giving 4.6 m wave height. Furthermore, the sensitivity test should apply a +10% increase on the 4.2 m wave height between 1990 and 2055, and apply a +10% increase on the 4.6 m wave height between 2056 and 2115.

Table 11. Offshore wind speed and extreme wave height allowance (with respect to 1990), valid around all the English coast. (Source: EA (2017))

Applies around all the English coast	1990 to 2055 (%)	2056 to 2115 (%)
Offshore wind speed allowance	+5	+10
Offshore wind speed sensitivity test	+10	+10
Extreme wave height allowance	+5	+10
Extreme wave height sensitivity test	+10	+10

It should be noted that there is a climate change project being carried out by the Environment Agency (EA) looking at the UK Climate Projections 2018 project. Data from the UK Climate Projections 2018 (UKCP18) project are expected to be available from November 2018.

2.4 Biological fouling

2.4.1 Characterisation of marine biological fouling

Marine biofouling, or biological fouling, is the undesirable growth of marine organisms (both plants and animals) on man-made structures that are submerged for a sustained period; e.g. boats, buoys, jetties and piers, and the bases of offshore installations such as oil rigs and wind turbine foundations. The species which cause biofouling are perfectly adapted to colonising naturally-occurring hard ***substrates***, such as rocky seashores; so the accumulation of marine growth on man-made structures is to some extent inevitable, despite ongoing advances in anti-fouling paints and coatings.

The life histories of biofouling species are characterised by a free-swimming or planktonic juvenile phase, which drifts on the ocean currents until it comes into contact with a suitable hard surface to colonise. The subsequent adult form attaches firmly to this surface and extracts nutrients from the water column. Common biofouling colonisers include barnacles, mussels, tubeworms, anemones and seaweed. More than 4000 biofouling species have been reported globally (*Cao et al., 2011*). The colonisation of ***sessile*** biofouling species then attracts mobile species such as fish and crustaceans.

Biofouling causes problems by increasing surface complexity, load and hydrodynamic drag on a structure. It can accelerate corrosion, compromise mechanical integrity and ultimately cause system failure. Whilst biofouling may be a concern for engineers, the creation of 'artificial reefs' can be a positive outcome in terms of habitat creation and biodiversity. Before the onset of industrial fisheries, large areas of the southern North Sea were covered in natural reefs, many of which are now lost (*Van der Stap et al., 2016*). In contrast, many thousands of artificial structures are now present in the North Sea in the form of shipwrecks, wind farms and oil and gas platforms; and thousands more will be installed in the near future.

Coastal power stations that utilise seawater in a *once-through cooling water system* can also suffer from biofouling within the system. If untreated this will impede water flow and drastically reduce the efficiency of heat transfer condensers. However, this is an offshore case study, so coastal power stations are given no further consideration here. They are discussed in Volume 11 – Marine Biological Fouling, and Case Study 3 — Hunterston.

2.4.2 Historical events and data

Offshore biofouling studies are reported in the literature. For example, *Forteath et al. (1982)* assessed marine growth on the North Sea oil platform Montrose Alpha. Marine growth samples were collected at five elevation levels during July and August between the years 1977 and 1980. In all, 45 different species were recorded, of which 40 were sessile forms. The greatest cover was found in the depth range from ***mean low water*** (MLW) to –31m below MLW, and the least was found between –71m below MLW and the mud-line (at –91m below MLW). The species that dominated biofouling at the different depths are shown in *Table 12*.

Table 12. Species dominating biofouling at different depths on the North Sea oil platform Montrose Alpha (Forteath et al., 1982).

Depth	Biofouling species
Sunlit surfaces (MLW to −10 m)	Large amounts of seaweed and kelp. Some plants reached a length of 2.5 m but most were about 1.5 m. The common mussel (*Mytilus edulis*) did not form beds but individuals were scattered amongst the seaweeds, many of them overgrown by ***epiphytes***.
−10 m to −31 m	The seaweeds rapidly gave way to ***hydroids*** and ***bryozoans***.
−31 m to −51 m	***Arborescent*** bryozoans were steadily replaced by ***calcareous*** bryozoans.
−51 m to −71 m	The calcareous bryozoans were largely replaced by encrusting bryozoan species. Extensive mats of *Alcyonidium hirsutum* (Fleming) were formed. Small aggregations of tubeworms also became present at the lower depths.
−71 m to mud-line (−91 m)	In general, there was very little biofouling. Discrete masses of tubeworms and deep-water barnacles were present.

Van der Stap et al. (2016) assessed the biofouling ***assemblages*** on five gas platforms in the southern North Sea to investigate the effects of depth, and distance offshore. The five platforms were sited on a gradient of increasing distance (from 48 km to 177 km) offshore, and at depths of between 27 m and 43 m (*Figure 10*). In all, 30 different taxa were identified. The three platforms furthest offshore (P3 to P5) became fully covered with marine fouling at all depths, whereas some legs of P1 and P2 were not fully covered, suggesting that biofouling increased with distance from the shore. The abundance of marine fouling was also found to be depth-dependent, with an initial increase in species richness until 15 to 20 m deep and then a decrease below that.

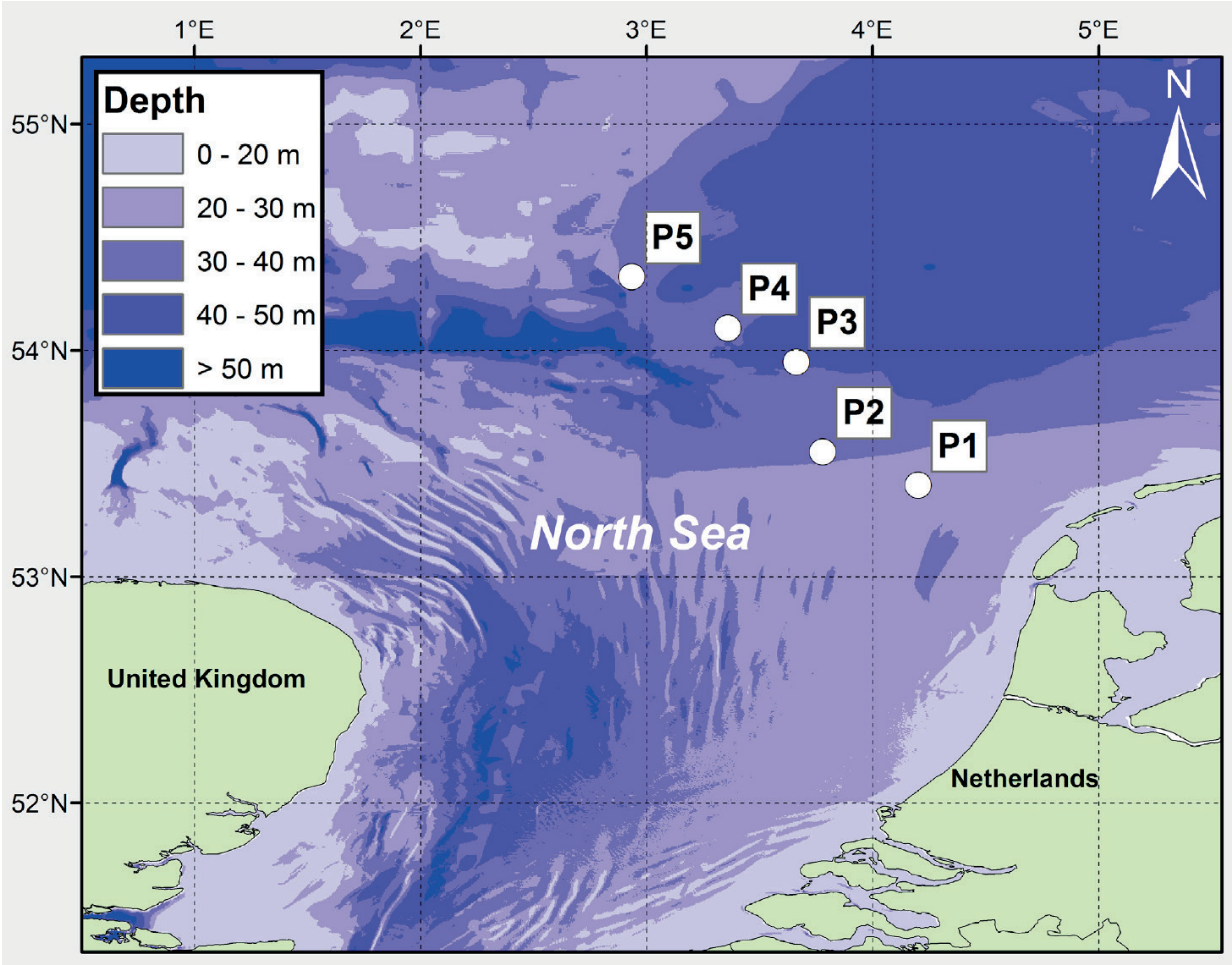

Figure 10. Locations of the platforms P1 to 5 (Van der Stap et al., 2016).

In the depth range 0 to 20 m, the blue mussel (*Mytilus edulis*) was often present, especially on P1 and P2. It was more abundant on P4 than P3 and P5, suggesting that the blue mussel is an early coloniser of offshore structures (P4 had been installed for three years, compared to seven years for P3 and 13 years for P5). The soft coral (*Alcyonium digitatum*) was only observed on platforms P3 to P5, suggesting that its abundance correlated positively with distance from shore, in line with the pattern found in shipwrecks in the Belgian part of the North Sea (*Zintzen and Massin, 2010*). Trends in other species were also found, but not all variability could be explained by depth or distance from the shore, indicating that other environmental variables play a role, e.g. salinity, water temperature, water currents, food supply, light penetration, silt content and the position on the leg (interior/exterior) in relation to the direction of the current.

During the recent decommissioning of piled wind turbines, from the Solway Firth (UK), hard fouling of up to 300 mm thickness was observed on the upper 2 to 3 m of the submerged structure (*Figure 11*).

Figure 11. Decommissioned wind turbine showing hard fouling of the upper 2 to 3 m of the submerged structure.

2.4.3 Assessing the hazard

The type and severity of biofouling depend on a range of interacting biological and physical parameters including sea water temperature, depth, light levels, turbidity, hydrodynamics, the biogeographical range of biofouling species, food availability, interspecific competition and predation.

In Volume 11 — Marine Biological Fouling, a literature review of the biological species responsible for biofouling (and clogging) has been undertaken, along with their functional traits, larval duration, settling behaviour and any other information which might identify likely proliferation conditions. The spatial distribution of each species was mapped using the International Council for the Exploration of the Sea (ICES) statistical areas, and all the above information was entered into a database. In all, 62 species were identified in nine main biological groups. Some have been previously recorded as providing nuisance to existing power assets, whilst others are considered sufficiently likely to cause nuisance. This new dataset, published in 2016, is the most comprehensive and up-to-date tool for characterising this natural hazard.

To undertake such a hazard assessment, it is necessary to combine the species-specific data, from the database, with information on the planned infrastructure and its local environment. For Dounreay, 39 of the 62 species in the database have been identified as occurring in the same ICES statistical area. The next step is to consider the settling and proliferation requirements for each of these 39 species, and whether they will be met by the planned infrastructure and its location/environment, e.g. depth, temperature, salinity, wave energy levels and currents.

For example, the blue mussel (*Mytilus edulis*) spawns (produces larvae) between April and September. The larvae spend 30 to 81 days as zooplankton, drifting passively in the water column, so the settling period is May to December (temperature permitting). Once settled, the blue mussel thrives at depths between 0 and 10 m, and at temperatures between 5 and 20 °C. It requires a minimum salinity of only 5 Practical Salinity Units (PSU), so it can survive in estuaries and other low salinity environments. If the location of the planned infrastructure meets these requirements, colonisation by the blue mussel should be expected, with growth rates of up to 2 mm per month, and a life expectancy of 18 years. In contrast, the kelp species, *Laminaria hyperborea*, tolerates a wider depth range (between 3 and 47 m) but requires a higher minimum salinity (30 PSU), so will not survive in estuaries. Where the environmental conditions are right, it can grow at a rate of up to 30 cm per month and survive for 20 years. This type of analysis should be repeated for each of the relevant species to characterise the marine biofouling risk for offshore infrastructure sited near Dounreay.

The database of biofouling species is a useful tool to start assessing the risks of marine biofouling to new marine or coastal infrastructure. However, this work should be considered as a snapshot of the information available at the time of publication (2016). The marine biological environment is inherently dynamic and future changes to water temperatures and circulation patterns, e.g. as a result of climate change, are expected to alter both native and non-native species distributions. Various observations have been made with respect to previously more southerly distributed species gradually extending their ranges northward as sea temperature averages increase. It is hoped that emerging power technologies will build upon this work, and that their future experiences of how fouling organisms affect new designs will add further useful information to the hazard dataset.

2.4.4 Mitigation

The prevalent strategy to manage the biofouling of offshore structures is the application of antifouling coatings, although these have typically been developed for ship hulls. However, a wide range of alternative methods is already being used on a smaller scale or currently being researched and developed. Some examples are described below.

A surface can be protected by being made into an anode, often done by forming a thin layer of platinum on the surface. An electric current of 5 mA/cm^2 was found to restrict fouling growth considerably for a long duration of time. Low power pulsed laser irradiation has also been shown to significantly lower the settlement rate of bacteria, micro algae, and the larvae of biofouling organisms. However, this method is relatively new and not widely used (*Nandakumar and Yano, 2003*).

Another form of antifouling is the use of biological enzymes. Some organisms can secrete enzymes or metabolites to inhibit the growth of their competitors. These secretions have a low toxicity and are biodegradable. Researchers have attempted to extract high concentrations of these secretions to be used for biological antifouling. Two types of enzymes are considered for antifouling: there are enzymes which degrade adhesives, which are effective at preventing macro-organism biofouling; and enzymes that interfere with intercellular communication, that effectively prevent micro-organism biofouling. A combination of both enzymes has been found to produce the best results. This is a new concept which requires further trials before being commercially used (*Cao et al., 2011*).

The antifouling abilities of vibration methods, such as acoustic technology, have also been confirmed. Hydroids, barnacles and mussels can be inhibited to some extent by either external vibration sources or piezoelectric coatings. However, the huge power consumption of these methods makes them less suitable.

Finally, other studies have evaluated magnetic fields, ultraviolet radiation and radioactive coatings. However, these methods are not yet in practical application (*Cao et al., 2011*).

This case study has provided an example of how methods in the technical volumes for a variety of hazards (here, extreme wind, extreme precipitation, coastal/offshore flooding and biological fouling) could be applied to the Dounreay site and surroundings. It also provides an example of how the technical approaches could be used to characterise the natural hazard risk at offshore sites elsewhere in the UK.

The study of extreme rainfall and wind presented here for Dounreay was based on observed mean daily wind speed and observed total daily rainfall recorded at nearby weather stations (because of their longer data record than that at the Dounreay site). An extreme value distribution was fitted to both the mean daily wind speed and total daily rainfall, and return levels were estimated for AEPs of 0.5, 0.05 and 0.01 (equivalent to 1 in 2-year, 1 in 20-year and 1 in 100-year return periods). Two distinct extreme value distributions were fitted to wind and rainfall data respectively; a generalised extreme value distribution and a Poisson generalised Pareto distribution, to illustrate two standard approaches for EVAs.

For extreme mean daily wind speed, the illustrative EVA indicated return levels of 17.5 m/s, 22.1 m/s and 22.8 m/s (with 95% confidence intervals of 16.9 to 18.1 m/s, 20.8 to 26.7 m/s and 21.2 to 29.5 m/s respectively) associated with AEPs of 0.5, 0.05 and 0.01 respectively. To place this analysis in some context, the wind speed recorded on the windiest day at Dounreay is 20.6 m/s on 2nd March 1970 (based on 14 years of observed data, for the period 1969 to 1983).

For rainfall, the EVA model chosen meant that the AEPs were dependent on the values of the standardised NAO index used as a covariate. In general, the smaller the standardised NAO index, the larger the expected return levels. However, the EVA model as specified was found to potentially underestimate the observed return levels of rainfall at the Dounreay site. This suggests that the EVA model may not be capturing certain physical processes, possibly because it assumes that the climate is stationary (i.e. longer-term changes in climate are not necessarily captured). The model chosen also did not take into account the effect of correlation between successive observations of rainfall.

The characterisation of tornadoes presented in this case study gives a 0.000001 AEP of any location in the UK being affected by a T0 to T3 intensity tornado (where these intensity categories account for ~95% of the tornadoes observed in the UK over the period 1981 to 2010). The method presented in this case study defines a site-specific calculation approach using a Poisson process, which accounts for the location and size of the area of interest. Using this approach, it is estimated that a tornado of intensity T3 or above in the Dounreay area is approximately a 1 in 200,000-year event whereas a tornado of intensity T5 or above would be a 1 in 6,500,000-year event. However, it is important to note that any analysis of observed UK tornadoes may be affected by potential issues with under-reporting, and the fact that the length of the observational record is several orders of magnitude shorter than the return periods quoted here. Although much progress in tornado research has been made by the Tornado and Storm Research Organisation in the past few decades, a longer observational record would allow more accurate estimates to be made for tornado return periods across the UK.

The impacts of snowfall, humidity, dust and sandstorms on onshore energy infrastructure are briefly described where guidance is available, and examples of offshore guidance standards are listed where appropriate. This document includes: (i) guidance on energy infrastructure standards required to withstand extremes in snow depth and ice build-up, (ii) a description of extreme humidity impacts, including loss of visibility and the effects of moisture ingress on offshore wind turbines, and (iii) a description of when airborne dust or sand falls in the UK, although the risk to Dounreay is relatively small because dust and sand fall normally originates from the south. Equally, it is not possible to define the localised impacts of falls of Saharan sand/dust without reliable observation records. Future changes in sand and dust storms depend on climate change scenarios for precipitation, winds and temperature as well as future land use changes which will determine how dust is transported from the source region. Probabilistic future projections (UKCP09) indicate that no clear statement can be made about future changes in snowfall or humidity at Dounreay.

For flood risk assessment at coastal, estuarine and offshore installations, both wind speed and wave height should ideally be analysed. An illustration of offshore wave buoy data has been provided alongside adjustments that should be made to account for climate change. The percentage increases in wind speed and extreme wave height shown in *Table 11* should be applied in a way that considers the accumulative effect over time. For example, for a 1 in 100-year (1% AEP) event, if the wave height is 4 m at the baseline year of 1990, then the 5% allowance (i.e. 0.2 m) should be added to the 4 m wave height during 1990 and 2055, giving 4.2 m wave height; and subsequently a further 10% allowance (i.e. 0.4 m) should be added to the 4.2 m wave height between 2056 and 2115, giving 4.6 m wave height. Furthermore, the sensitivity test should apply a +10% increase on the 4.2 m wave height between 1990 and 2055 and apply a +10% increase on the 4.6 m wave height between 2056 and 2115.

3. Conclusions

Where the effects of biological fouling are identified (i.e. an undesirable accumulation of micro- and macro-organisms on artificial surfaces immersed in water), it has been shown to have the potential to influence the loading of offshore structures by:

- increasing the size of structural elements;
- increasing the drag and inertia coefficients;
- increasing the structural weight;
- potentially accelerating corrosion;
- damaging protective coating and interfering with sensitive areas necessary for monitoring and maintenance.

Biofouling mechanisms are influenced by numerous factors such as depth in water, water flow, water quality, availability of light and surface area topography, as well as local variations in the biofouling species. Examples relating to the Dounreay area have been presented and it has been noted that a full characterisation of the marine biofouling hazard here would require the study of 39 different species. However, the database of biofouling species used here should only be seen as a snapshot of the current species in the Dounreay area (as of 2016), and it is suggested that this database is updated given the dynamic nature of marine environments.

The occurrence of biofouling in a marine environment is inevitable without mitigatory measures being taken, and a discussion has been presented as to the likely candidates for protection and mitigation. Antifouling strategies depend on the type of object being protected. Moving objects and platforms usually rely on coatings, while structures such as condenser tubing and cooling water intakes are protected by the addition of biocide into the water column. Environmentally friendly solutions are continuously being sought and are the subject of ongoing research. It is also noted that the technologies in use for controlling and/or removing biofouling communities offer opportunities for monitoring of local conditions and any changes that might occur over time.

Apsley ML, Mulder KJ, Schultz DM. 2016. Re-examining the United Kingdom's greatest tornado outbreak: forecasting the limited extent of tornadoes along a cold front. *Weather and Forecasting*, 31, 853–875. doi: 10.1175/WAF-D-15-0131.1

Ashcroft J. 1994. The relationship between the gust ratio, terrain roughness, gust duration and the hourly mean wind speed. *Journal of Wind Engineering and Industrial Aerodynamics*, 53, 331–355. doi: 10.1016/0167-6105(94)90090-6

BBC. 2003. Tornado spotted in Scotland. http://news.bbc.co.uk/1/hi/scotland/3098977.stm (accessed on 28th June 2018).

BBC. 2010. Mini tornadoes in Firth of Forth. http://news.bbc.co.uk/1/hi/scotland/edinburgh_and_east/8443441.stm (accessed on 28th June 2018).

Bech JI, Hasager CB, Bak C. 2018. Extending the life of wind turbine blade leading edges by reducing the tip speed during extreme precipitation events. *Wind Energy Science*, in review. doi: 10.5194/wes-2017-62

Boorman P, Jenkins G, Murphy J. 2010. *Future Changes in Fog Frequency from the UKCP09 Ensemble of Regional Climate Model Projections*. Available at: http://ukclimateprojections.metoffice.gov.uk/media.jsp?mediaid=87948&filetype=pdf (accessed on 28th June 2018).

Brown SJ. 2017. The drivers of variability in UK extreme rainfall. *International Journal of Climatology*, 38, e119–e130. doi: 10.1002/joc.5356

Brown SJ, Boorman P, Murphy J. 2010. *Interpretation and Use of Future Snow Projections from the 11-Member Met Office Regional Climate Model Ensemble*. Available at: http://ukclimateprojections.metoffice.gov.uk/media.jsp?mediaid=87949&filetype=pdf (accessed on 28th June 2018).

Cao S, Wang JD, Chen HS, Chen DR. 2011. Progress of marine biofouling and antifouling technologies. *Chinese Science Bulletin*, 56, 598–612. doi: 10.1007/s11434-010-4158-4

Cefas. 2018. Wavenet. https://www.cefas.co.uk/cefas-data-hub/wavenet/ (accessed on 28th June 2018).

Chan SC, Kahana R, Kendon EJ, Fowler HJ. 2018. Projected changes in extreme precipitation over Scotland and Northern England using a high-resolution regional climate model. *Climate Dynamics,* 1–19. doi: 10.1007/s00382-018-4096-4

Coles S. 2001. *An Introduction to Statistical Modelling of Extreme Values,* Springer, London, UK.

Collier CG, Fox NI, Hand WH. 2002. *Extreme Rainfall and Flood Event Recognition.* R&D Technical Report FD2201. DEFRA/Environment Agency. Available at: http://sciencesearch.defra.gov.uk/Document.aspx?Document=FD2201_708_TRP.pdf (accessed on 28th June 2018).

EA. 2017. Flood risk assessments: climate change allowances. https://www.gov.uk/guidance/flood-risk-assessments-climate-change-allowances (accessed on 28th June 2018).

Elsom DM, Meaden GT. 1982. Suppression and dissipation of weak tornadoes in metropolitan areas: a case study of greater London. *Monthly Weather Review,* 110, 121–132. doi: 10.1175/1520-0493(1982)110<0745:SADOWT>2.0.CO;2

European Commission. 2000. *Directive 2000/60/EC of the European Parliament and of the Council of 23 October 2000 Establishing a Framework for Community Action in the Field of Water Policy.* Available at: https://publications.europa.eu/en/publication-detail/-/publication/70e52c10-85a1-4e97-8218-ed56d597ed05/language-en (accessed on 28th June 2018).

Evening Express. 2016. Spectacular funnel cloud forms off Aberdeen coast. https://www.eveningexpress.co.uk/fp/news/local/spectacular-funnel-cloud-forms2 (accessed on 28th June 2018).

Evening Express. 2017a. Possible tornado caught on camera near Aberdeen. https://www.eveningexpress.co.uk/fp/news/local/watch-possible-tornado-caught-camera-near-aberdeen (accessed on 28th June 2018).

Evening Express. 2017b. This might look like a tornado forming over Inverurie, but it's not. https://www.eveningexpress.co.uk/fp/news/local/watch-this-might-look-like-a-tornado-forming-over-inverurie-but-its-not/ (accessed on 28th June 2018).

Ferro CAT, Segers J. 2003. Inference for clusters of extreme values. *Journal of the Royal Statistical Society: Series B (Statistical Methodology),* 65, 545–556. doi: 10.1111/1467-9868.00401

Forteath G, Picken G, Ralph R, Williams J. 1982. Marine growth studies on the North Sea oil platform Montrose Alpha. *Marine Ecology Progress Series,* 8, 61–68.

Gilleland E, Katz RW. 2016. extRemes 2.0: an extreme value analysis package in R. *Journal of Statistical Software,* 72, 1–39. doi: 10.18637/jss.v072.i08

Hewston R, Dorling SR. 2011. An analysis of observed daily maximum wind gusts in the UK. *Journal of Wind Engineering and Industrial Aerodynamics,* 99, 845–856. doi: 10.1016/j.jweia.2011.06.004

HI-energy. 2018. HI-energy website. http://www.hi-energy.org.uk/ (accessed on 28th June 2018).

Holden J, Wright A. 2004. UK tornado climatology and the development of simple prediction tools. *Quarterly Journal of the Royal Meteorological Society,* 130, 1009–1021. doi: 10.1256/qj.03.45

Holley DM, Dorling SR, Steele CJ, Earl N. 2014. A climatology of convective available potential energy in Great Britain. *International Journal of Climatology,* 34, 3811–3824. doi: 10.1002/joc.3976

HSE. 2002. *Environmental Considerations.* Offshore Technology Report 2001/010. Available at: http://www.hse.gov.uk/research/otopdf/2001/oto01010.pdf (accessed on 28th June 2018).

IPCC. 2013. *Climate Change 2013: The Physical Science Basis.* Contribution of Working Group I to the Fifth Assessment Report of the Intergovernmental Panel on Climate Change. Cambridge University Press, Cambridge, UK.

Jones AM. 1975. The marine environment of Orkney. In *The Natural Environment of Orkney, Proceedings of the Nature Conservancy Council symposium held in Edinburgh, 26–27 November 1974.* Nature Conservancy Council, Edinburgh, UK.

Kendon EJ, Roberts NM, Fowler HJ, Roberts MJ, Chan SC, Senior CA. 2014. Heavier summer downpours with climate change revealed by weather forecast resolution model. *Nature Climate Change*, 4, 570–576. *doi: 10.1038/nclimate2258*

Kirk PJ. 2007. UK tornado climatology 1980–2004. *The International Journal of Meteorology*, 32, 158–172.

Kirk PJ. 2014. An updated tornado climatology for the UK: 1981–2010. *Weather*, 69, 171–175. *doi: 10.1002/wea.2247*

LGA. 2018. Managing flood risk. *https://www.local.gov.uk/topics/severe-weather/flooding/flood-and-coastal-erosion-risk-management/managing-flood-risk* (accessed on 28th June 2018).

MarLIN. 2018. MarLIN — The Marine Life Information Network. *https://www.marlin.ac.uk* (accessed on 28th June 2018).

Meaden GT. 1985. *A Study of Tornadoes in Britain with Assessments of the General Tornado Risk Potential and the Specific Risk Potential at Particular Regional Sites.* Tornado and Storm Research Organisation, Bradford-on-Avon, UK.

Met Office. 2018a. Tornado. *https://www.metoffice.gov.uk/learning/wind/tornado* (accessed on 28th June 2018).

Met Office. 2018b. Humidity. *https://www.metoffice.gov.uk/learning/learn-about-the-weather/weather-phenomena/humidity* (accessed on 28th June 2018).

Mizuta R. 2012. Intensification of extratropical cyclones associated with the polar jet change in the CMIP5 global warming projections. *Geophysical Research Letters*, 39, L19707. *doi: 10.1029/2012GL053032*

Mulder KJ, Schultz DM. 2015. Climatology, storm morphologies, and environments of tornadoes in the British Isles: 1980–2012. *Monthly Weather Review*, 143, 2224–2240. *doi: 10.1175/MWR-D-14-00299.1*

Nandakumar K, Yano T. 2003. Biofouling and its prevention: a comprehensive overview. *Biocontrol Science*, 8, 133–144. doi: 10.4265/bio.8.133

NDA. 2014. *Strategic Environmental Assessment — Site Specific Baseline Dounreay.* Available at: http://webarchive.nationalarchives.gov.uk/20100806155332/http://www.nda.gov.uk/strategy/sea08.cfm (accessed on 28th June 2018).

Perry M, Hollis D. 2005. The generation of monthly gridded datasets for a range of climatic variables over the UK. *International Journal of Climatology*, 25, 1041–1054. doi: 10.1002/joc.1161

Pitt M. 2008. *The Pitt Review: Learning Lessons from the 2007 Floods.* Available at: http://webarchive.nationalarchives.gov.uk/20100702215619/http://archive.cabinetoffice.gov.uk/pittreview/thepittreview/final_report.html (accessed on 28th June 2018).

Prahl BF, Rybski D, Burghoff O, Kropp JP. 2015. Comparison of storm damage functions and their performance. *Natural Hazards Earth System Science*, 15, 769–788. doi: 10.5194/nhess-15-769-2015

Ranakoti R. 2003. Presentation on offshore platform design. Available at: https://www.slideshare.net/rahulranakoti/offshore-platformdesign (accessed on 28th June 2018).

Raynor GS. 1978. Effects on atmospheric diffusion of meteorological processes in coastal zones. In *Air Quality Meteorology and Atmospheric Ozone*, ASTM International. doi: 10.1520/STP36587S

Rocha-Lima A, Martine JV, Remer LA, Todd M, Marsham JH, Engelstaedter S, Ryder CL, Cavazoa-Guerra C, Artaxo P, Colarco P, Washington R. 2018. A detailed characterisation of the Saharan dust collected during the Fennec campaign in 2011: in situ ground-based and laboratory measurements. *Atmospheric Chemistry and Physics*, 18, 1023–1043. doi: 10.5194/acp-18-1023-2018

Scottish Government. 2011. Scotland's Marine Atlas: Information for The National Marine Plan. http://www.gov.scot/Publications/2011/03/16182005/23 (accessed on 28th June 2018).

Scottish Government. 2017. Scottish Energy Strategy: The future of energy in Scotland. *https://www.gov.scot/energystrategy* (accessed on 28th June 2018).

SEPA. 2018. Flood maps. *https://www.sepa.org.uk/environment/water/flooding/flood-maps/* (accessed on 28th June 2018).

Sexton DMH, Murphy J. 2010. *UKCP09: Probabilistic Projections of Wind Speed.* Available at *http://ukclimateprojections.metoffice.gov.uk/media.jsp?mediaid=87876&file?type=pdf* (accessed on 28th June 2018).

Silverman BW. 1986. *Density Estimation for Statistics and Data Analysis,* Monographs on Statistics and Applied Probability, Chapman and Hall, London, UK.

The Highland Council. 2010. *Highland Coastal Development Strategy.* Available at: *http://www.highland.gov.uk/download/downloads/id/1062/highland_coastal_development_strategy.pdf* (accessed on 28th June 2018)

The Scotsman. 2013. Mini-tornado spotted in Scotland. *https://www.scotsman.com/news/environment/mini-tornado-spotted-in-scotland-1-2974493* (accessed on 28th June 2018).

Van der Stap T, Coolen JWP, Lindeboom HJ. 2016. Marine fouling assemblages on offshore gas platforms in the southern North Sea: Effects of depth and distance from shore on biodiversity. *PLoS One,* 11, 19–21. *doi: 10.1371/journal.pone.0146324*

WMO. 1966. *International meteorological vocabulary.* WMO, No. 182. TP. 91. Geneva, Switzerland. pp. xvi, 276. Sw. fr. 40.

WMO. 2018. Sand and dust storms. *https://public.wmo.int/en/our-mandate/focus-areas/environment/sand-and-dust-storm* (accessed on 28th June 2018).

Zappa G, Shaffrey L, Hodges KI, Sansom PG, Stephenson DB. 2013. A multimodel assessment of future projections of North Atlantic and European extratropical cyclones in the CMIP5 climate models. *Journal of Climate,* 26, 5846–5862. *doi: 10.1175/JCLI-D-12-00573.1*

Zhang S. 2017. When a hurricane hits an offshore oil platform. *https://www.theatlantic.com/science/archive/2017/08/harvey-offshore-platform-oil-gas/537960/* (accessed on 28th June 2018).

Zintzen V, Massin C. 2010. Artificial hard substrata from the Belgian part of the North Sea and their influence on the distributional range of species. *Belgian Journal of Zoology,* 140, 20–29.

Arborescent
Resembling a tree.

Assemblage
A collection or gathering.

Bathymetry
Depth of water in estuaries, coasts, oceans, seas and lakes; generally surveyed with reference to chart datum.

Bryozoans
Colonies of microscopic animals; the colonies of different species take different forms.

Calcareous
Composed of, or containing, calcium carbonate, calcium or limestone.

Dry-bulb temperature
The temperature of air as measured by a thermometer freely exposed to the air, but shielded from moisture and radiation typically by a Stevenson screen.

Epiphytes
Organisms that grow on the surface of a plant.

Hydroids
Colonies of microscopic animals (polyps, or inverted jellyfish) attached to a feather-like base, often mistaken for plants.

Mean low water (MLW)
The average water level between low tides at springs and neaps.

Modes of variability
A climate pattern that has a set pattern of spatial and temporal behaviour, typically affecting specific regions and over seasonal or longer timescales. This behaviour occurs on a quasi-regular basis. Examples of modes of variability include the North Atlantic Oscillation, El Niño-Southern Oscillation and the Atlantic Multi-decadal Oscillation.

Noise (statistical)

The unexplained variability present within a sample of data.

North Atlantic Oscillation (NAO)

A large-scale surface pressure gradient between the 'Azores high' and 'Icelandic low'. A positive NAO represents a large pressure difference with stronger westerly winds whereas a negative NAO represents a smaller pressure difference and therefore weaker westerly winds.

Once-through cooling water system

Extracts cold water from the environment, circulates it through pipework and condensers to absorb heat from other systems, e.g. steam turbines, and then discharges the warmed-up water back to the environment. The opposite of a closed system, in which the water is recirculated.

Ordnance datum

The mean sea level as defined for Ordnance Survey; mean sea level calculated from observations taken at Newlyn, Cornwall, and used as the official basis for height calculation on British maps.

Sessile

Fixed in one place; immobile.

Substrate

The surface or material on which an organism lives and grows.

Wet-bulb temperature

The temperature of air measured using a thermometer wrapped in wet muslin, representing the adiabatic saturation temperature.

Abbreviations

AOD	Above ordnance datum
AEP	Annual exceedance probability
ASL	Above sea level
AWI	Ancient Woodland Inventory
Cefas	Centre for Environment, Fisheries and Aquaculture Science
EA	Environment Agency
EMEC	European Marine Energy Centre
EVA	Extreme value analysis
GEV	Generalised extreme value
GMT	Greenwich Mean Time
GPD	Generalised Pareto distribution
ICES	International Council for the Exploration of the Sea
MarLIN	The Marine Life Information Network
MLW	Mean low water
NAO	North Atlantic Oscillation
NCIC	National Climate Information Centre
PP-GPD	Point-process generalised Pareto distribution
PSU	Practical Salinity Units
SAC	Special Area of Conservation
SEPA	Scottish Environment Protection Agency
SPA	Special Protection Area
SSSI	Site of Special Scientific Interest
TORRO	Tornado and Storm Research Organisation
UKCP09	United Kingdom Climate Projections 2009
UKCP18	United Kingdom Climate Projections 2018

A.1 EVA

An extreme value analysis (EVA) is a statistical technique designed to quantify the magnitude of natural hazard events and to estimate the likelihood of their occurrence using observed data (*Coles, 2001*). It also allows a robust quantification of the associated uncertainty in the analyses. EVA is used in this case study to estimate the return periods of extreme wind and extreme rainfall events. A return level is associated with an annual exceedance probability (AEP) and is the value (e.g. a wind speed value) that has the specified probability of being exceeded in a one-year period. A return period is the inverse of the AEP, and it is the expected number of events that will occur in a set period of time, assuming that the time series used has no systematic trends or oscillations.

An EVA is a statistical approach that models only the most extreme values in an observational record and provides a framework for quantifying and extrapolating out to extreme levels beyond those seen in the observational record. See Volume 1 — Introduction to the Technical Volumes and Case Studies, Volume 3 — Extreme Wind, and Volume 4 — Extreme Precipitation for more details.

Typically, two approaches are used to select a subset of extreme events to analyse them. These are:

Block maxima

The idea is to select the largest observation in a given time block and then fit a generalised extreme value (GEV) distribution to those extremes. For environmental data, a block is often chosen as a year, as this takes into account seasonal variability. A GEV analysis is usually applied to data where the extreme events are defined as the most extreme within a fixed time period. However, one of the issues with using a block maxima approach to select extreme events is that only the most extreme value within the block is selected, ignoring potentially informative but less extreme events.

Threshold exceedance model

A threshold exceedance model is applied only to observations which fall beyond a specified threshold. As a result, there may be several or no extreme observations in a given time block. A form of the generalised Pareto distribution (GPD) is then fitted to these data. The downside of the threshold approach is that the choice of the threshold can be difficult and subjective (see Volume 1 — Introduction to the Technical Volumes and Case Studies). The threshold must separate the extreme values from the main body of data. Too low a threshold leads to too many events classified as extreme, some of which have statistical characteristics that are more suitable to the main body of the data. Too high a threshold could result in too few extreme events from which to establish the appropriate values of the distribution parameters. Both of these outcomes could result in the fit of the distribution being poor. Within the meteorological community, typically either a GPD or a point-process GPD, also referred to as a Poisson-GPD (PP-GPD) (see Volume 3 — Extreme Wind and Volume 4 — Extreme Precipitation for more details), can be used to analyse the wind speed or rainfall data.

Note that extreme wind speed and extreme rainfall can be analysed using either a block maxima or threshold exceedance approach. The GEV (or block maxima) approach is a more practical method to apply to variables which are highly autocorrelated (i.e. where there is temporal dependence between data points). Both approaches are demonstrated in this case study: the GEV is illustrated with extreme wind data (see *Section 2.1.2*), and the PP-GPD approach is illustrated with rainfall data (see *Section 2.1.3*).

Either approach can be implemented, as done in this case study, with the extRemes EVA package in the statistical programming language R (*Gilleland and Katz, 2016*). Other software packages also contain code that can be used for EVA.

For simplicity, the illustrative analysis for wind and rainfall in this case study assumes that there is no long-term climate change trend present in these data. Section 6 of Volume 3 — Extreme Wind discusses the impacts of climate change on extreme wind speeds and rainfall by providing references to the appropriate literature, as well as how to incorporate these trends into an EVA.

A.2 Data requirements

Weather stations near to Dounreay are shown in *Figure 12*. All weather stations are classed as land-based weather stations (including Sule Skerry which is based on an island ~70 km off the coastline of Dounreay). Data recorded include daily rainfall, daily mean wind speed and daily maximum gust (gusts are defined in Volume 3 — Extreme Wind). However only daily mean wind speed and daily rainfall will be used in subsequent analyses in this case study.

To estimate the probability of any extreme events with an EVA, a long record (i.e. at least 30 years) of data is needed. Too short a record would lead to the under- or over-estimation of the return levels. A long record increases the probability of sampling rare events and provides some estimation of the uncertainty associated with such an analysis. It would also include the effect of naturally-occurring ***modes of variability***, such as the NAO (see Volume 3 — Extreme Wind).

The NAO is known to affect extreme precipitation and wind speed events.

Observations of wind speed (daily means) and rainfall (daily totals) are available for the Dounreay site from January 1969 to February 1983 and from January 1961 to June 1983 respectively (i.e. approximately 14 and 22 years). This record is too short to estimate AEP of less than 0.05 (greater than a 1 in 20-year return period) as required in this case study.

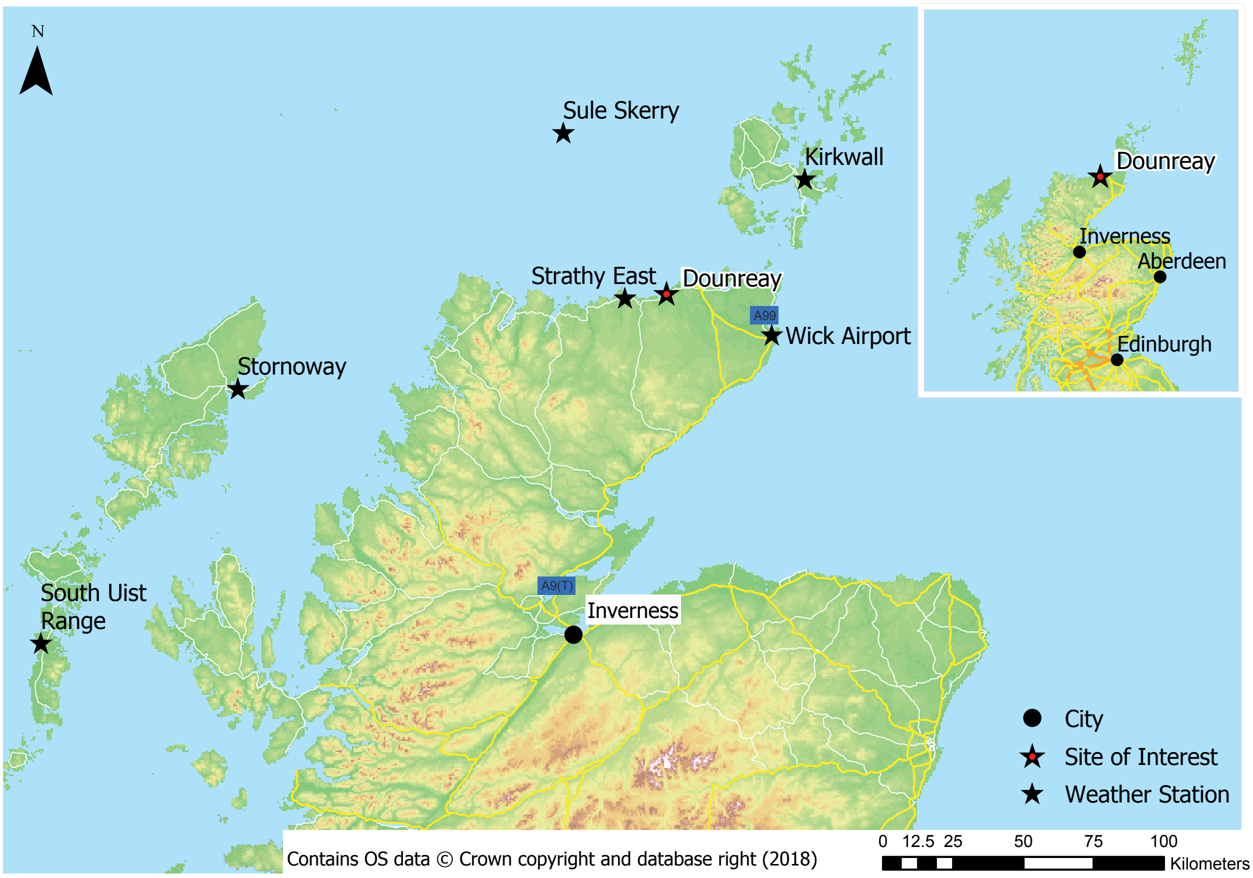

Figure 12. Map showing the locations of meteorological observation data available at and near Dounreay. (Source: contains OS data © Crown copyright and database right (2018))

When a sufficiently long record is not available, as is the case for Dounreay, there are a number of different approaches that can be used. These include:

- choosing a nearby weather station that has the required period of data and a similar climatology to Dounreay;
- infilling missing observations or extending the length of Dounreay's record by using observations from a nearby weather station with a similar climatology;
- using a weighting approach to create a blended record (weather stations are weighted according to a metric). Possible weight metrics could be the distance from Dounreay or the correlation between Dounreay's data and the nearby weather station's data;

- including the other weather stations as covariates in an EVA. The reader will note that this increases significantly the complexity of the analysis as referred to in Volume 3 — Extreme Wind and Volume 4 — Extreme Precipitation.

In this case study, the most pragmatic approach (choosing a nearby weather station) is adopted. *Table 13* shows a list of alternative weather stations, all close to Dounreay. Three of them have a record longer than 45 years for both wind speed and rainfall (Wick Airport, Kirkwall and Stornoway).

The weather station with the most similar climatology need not be the closest; for example, although Wick Airport is geographically closest to Dounreay, it does not necessarily imply that it will have a similar climatology. Wick is located on the east coast and appears to be sheltered from the more extreme south-westerly winds.

To identify the weather station most similar to Dounreay, the record of each nearby weather station is subsetted to the same period as that of Dounreay (1969 to 1983 for wind speed; 1961 to 1983 for rainfall). This ensures that the data encompass the same phases of long-term naturally-occurring modes of climate variability (e.g. the NAO). The extreme events of each weather station are then selected and compared with those of Dounreay (e.g. top 40 most extreme wind speeds at Wick Airport from 1969 to 1983 with the top 40 most extreme wind speeds at Dounreay). The mean squared deviation between those is calculated and the weather station with the lowest mean squared deviation overall (the least different extremes) is chosen as the most comparable weather station to Dounreay for the considered meteorological variable. The most comparable weather station's entire record can then be used in any subsequent analysis. This approach was adopted for selecting the most comparable weather station to Dounreay for wind data and rainfall data (see *Sections 2.1* and *2.2*).

*Table 13. Data available from weather stations near Dounreay. *Daily rainfall is measured from 09:00 GMT to 09:00 GMT on the next day. (© Crown Copyright Met Office 2018)*

Weather station (altitude)	Distance from Dounreay (km)	Daily mean wind speed (knots)		Daily maximum gust speed (knots)		Daily rainfall* (mm)	
		Period of data availability	Completeness of available data record (%)	Period of data availability	Completeness of available data record (%)	Period of data availability	Completeness of available data record (%)
Dounreay (21 m)	0	1969 to 1983	90.3	1973 to 1983	90.6	1961 to 1983	98.5
Wick Airport (36 m)	~40	1965 to 2018	97.9	1973 to 2018	96.9	1961 to 2018	98.9
Kirkwall (26 m)	~64	1969 to 2018	98.5	1973 to 2018	97.9	1961 to 2018	98.6
Sule Skerry (12 m)	~68	No data	N/A	1997 to 2018	64.0	1961 to 1980	98.7
South Uist Range (4 m)	255	1996 to 2018	95.9	1996 to 2018	96.3	1996 to 2018	93.1
Stornoway Airport (15 m)	156	1957 to 2018	98.9	1973 to 2018	98	1930 to 2018	99.9

A.3 Advanced EVA for extreme daily rainfall including NAO covariate

A.3.1 Fitting a PP-GPD model that includes a covariate for the NAO

The following diagnostic plots (*Figure 13*) investigate whether including the NAO, as a covariate in the location parameter, led to an improvement in the fit of the PP-GPD model described in *Section 2.2*. (Volume 4 — Extreme Precipitation provides a brief description on using covariates in an EVA.)

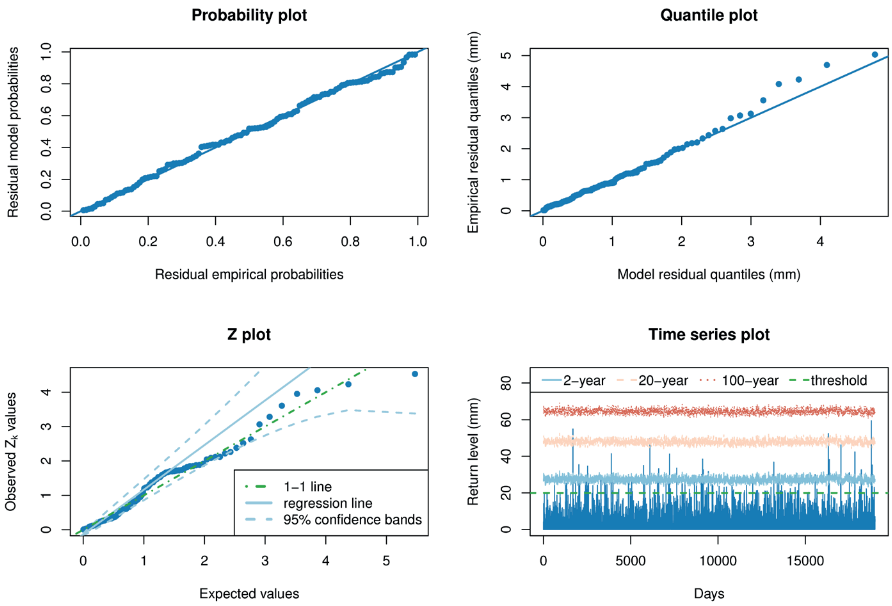

Figure 13. Diagnostic plots of the fit of the PP-GPD distribution to the extreme rainfall daily totals at Wick with the NAO index as covariate. The top plots show the fit residuals against the model residuals. The confidence intervals are approximate 95% normal confidence intervals.

AEPs derived from this model are now dependent on both the frequency (or rarity) of the extreme daily rainfall totals and the phase of the NAO. As a result, the probability plot (top left) and the quantile plot (top right) use the fitted residuals (*Coles, 2001*), and effective return levels are provided in the time series plot (bottom right). Effective return levels are the return levels that would be estimated from the fitted PP-GPD using the reported daily value of the NAO index.

The inclusion of NAO as a covariate has led to a better correspondence of the model probabilities to the empirical probabilities (top left plot *Figure 13*) compared to the PP-GPD without the covariate (top left *Figure 7*) and as a result the suggestion that the fitted model underestimates the observed data is considerably reduced, and may only be present for the most extreme events.

The Z plot highlights that there might still be issues with the fit of the PP-GPD, as the observations systematically deviate from the fitted regression line. The Z plot assess the suitability of the PP-GPD model (the PP component) in modelling the frequency of the extreme rainfall events. If the extreme rainfall observations are independent of one another, then the regression line through these observations (solid line) will align with the 1:1 line (dashed dotted line). A well fitting model should have a large percentage of extreme values lying within the 95% confidence interval (calculated using a normal approximation) of the fitted regression line (dashed lines). One possible explanation is that the current fitted PP-GPD model assumes that the observations of extreme rainfall are independent of one other. This initially seemed a reasonable assumption as over 90% of the extreme observations were separated by more than 10 days. However, as a result of the systematic deviation in this Z plot, it may now be desirable to investigate the sensitivity of the analysis to this assumption or to other factors which could cause extreme rainfall events to occur in clusters, such as seasonality.

More formally, a likelihood ratio test can be used to compare the PP-GPD model without NAO as a covariate to the model with NAO as a covariate in the location parameter. The *p*-value obtained is less than 0.02, implying that the inclusion of the NAO in the location parameter gives a better fitting model (statistically significant at the 5% significance level), and confirms that a PP-GPD with NAO as a covariate is an improvement upon the PP-GPD model fitted without a covariate in *Section 2.2*.

The time series plot shows the rainfall totals (dark blue) along with the 'effective' return levels. Daily rainfall return levels associated with AEPs of 0.5, 0.05 and 0.01 (1 in 2-year, 1 in 20-year and 1 in 100-year return periods) are shown in pale blue, pale orange and dark orange respectively. As shown in the plot, there is some variability associated with the total daily rainfall amounts for each return period shown. This variability is a direct result of the dependency in the PP-GPD model on the NAO index as a covariate.

For a given value of the NAO index, it is possible to derive NAO-specific AEPs. *Table 14* shows return levels for AEPs of 0.5, 0.05 and 0.01 conditioned on standardised values of the NAO, along with associated 95% confidence intervals. The largest rainfall totals generally occur when the NAO index is large and negative which is broadly in agreement with the results from *Brown (2017)* who investigated the effects of NAO and climate change on rainfall gridded data for London. However, care should be taken with the interpretation of the rainfall return levels in the table, as these are the AEPs for specific values of the NAO index and are calculated assuming that the specific NAO is fixed at a constant value for each day of the year, which is not the case. For example, the daily rainfall total has a 50% chance of being greater than 32 mm in a single year only if the NAO index is –3 for all days in that year.

Table 14. Daily rainfall total return levels (mm) associated with particular AEPs, along with 95% confidence intervals (calculated using the delta approach) given particular values of the NAO index. (© Crown Copyright Met Office 2018)

		Standardised NAO index						
		–3	–2	–1	0	1	2	4
AEP	0.5	32 (27, 36)	30 (27, 34)	29 (26, 31)	27 (25, 29)	26 (24, 28)	24 (21, 27)	23 (19, 27)
	0.05	52 (43, 62)	51 (42, 60)	49 (41, 58)	48 (39, 57)	46 (37, 55)	45 (36, 54)	43 (34, 53)
	0.01	70 (48, 90)	68 (46, 89)	66 (45, 87)	65 (43, 86)	63 (41, 87)	62 (40, 83)	60 (38, 82)

A.3.2 Further considerations

The analysis of extreme rainfall provided in this case study raised the following questions:

- How sensitive are the results to any dependency between observations of extreme rainfall? In other words, would similar return levels and confidence intervals be obtained if correlated daily rainfall data were removed (or if the analysis was adjusted to compensate for any correlation between extreme rainfall events)?
- What return level values should be used for a specific AEP if it is desirable to take into account the variability of the NAO index within a year?

Detailed analyses addressing these questions are not within the scope of this illustrative case study but possible approaches are described briefly below. The interested reader is also referred to the Trawsfynydd case study where these techniques are illustrated using temperature data.

Removing correlated extreme values

The PP-GPD models used both with and without the NAO as a covariate have assumed that the extreme values selected were independent of one another; an important assumption in the analysis of extreme values (see Section 5 of Volume 4 — Extreme Precipitation). In reality, there may be some autocorrelation present in the most extreme events and the extent of this autocorrelation should be assessed. Autocorrelation can be alleviated using a 'declustering' method. This assumes that consecutive exceedances of the 20 mm threshold belong to the same cluster and selects the maximum rainfall value in each cluster. A cluster starts when values go beyond the threshold and ends when they fall below this threshold for a set period of time (e.g. number of days). The number of days used to mark the end of a cluster is called the run length. Run lengths can either be specified based on physical knowledge or selected using an interval method such as that proposed by *Ferro and Segers (2003)*. Care should be taken when defining a run length and good practice would investigate the sensitivity of the EVA to the user-specified run length.

Calculating representative return levels

Instead of deriving the return levels given values of the NAO index and AEPs as shown in *Table 14*, a more realistic approach would be to take the average of the effective return levels for the desired AEP for each observation of the NAO index.

The disadvantage of such an approach is that only observed values of the NAO index are used and they may not be representative of the true NAO index distribution. Alternative approaches are either to fit a statistical distribution to the NAO indices, or to estimate the density of their distribution using density estimation techniques, e.g. kernel density estimation (*Silverman, 1986*). From these fitted distributions to the NAO data, a larger range of NAO indices could be sampled. A disadvantage of either of these approaches is that, as they are purely statistical, no account is taken of any physical bounds associated with the covariate (in this case, the likely range of the NAO index based on physical considerations). Case Study 1 — Trawsfynydd provides examples of representative return levels calculated by sampling the observed values of the NAO index and assuming the NAO data are normally distributed.

Appendix B: Wave graphs from WaveNet

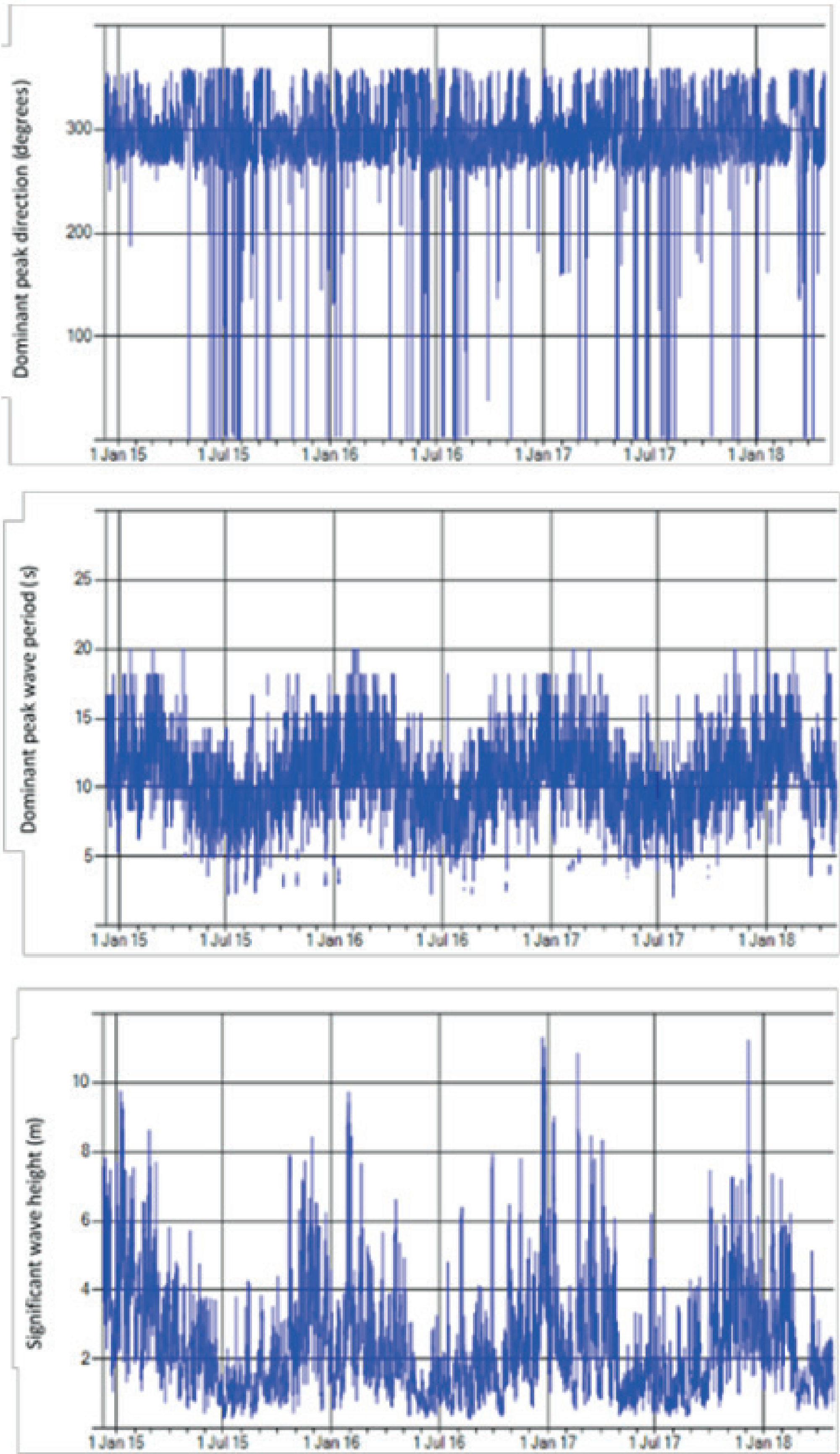

Figure 14. Wave data at Billia Croo: significant wave height, peak wave period and wave direction. (Source: EMEC hosted at Cefas (2018); © Crown Copyright 2018)

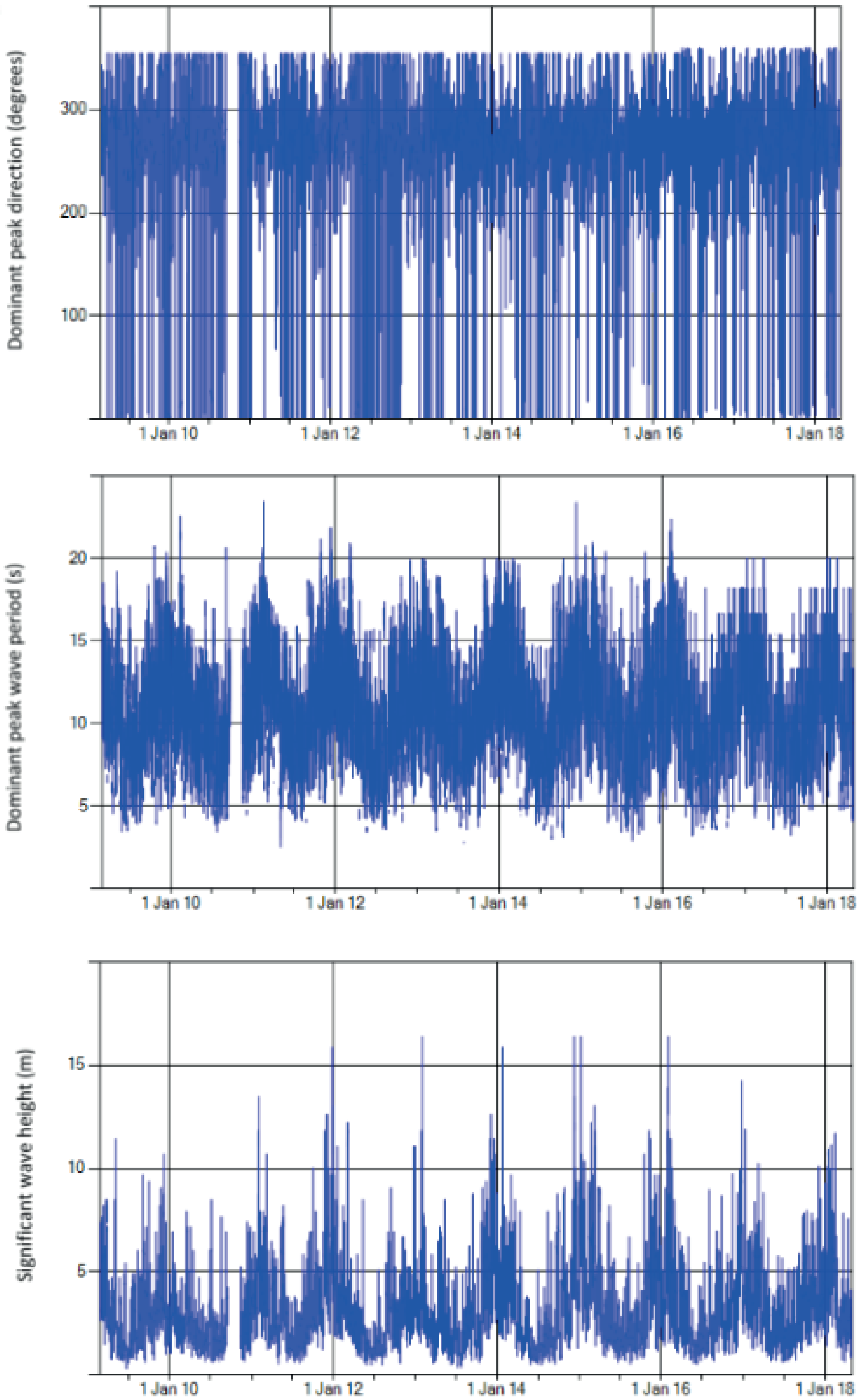

Figure 15. Wave data at West of Hebrides: significant wave height, peak wave period and wave direction. (Source: Cefas (2018); © Crown Copyright 2018)

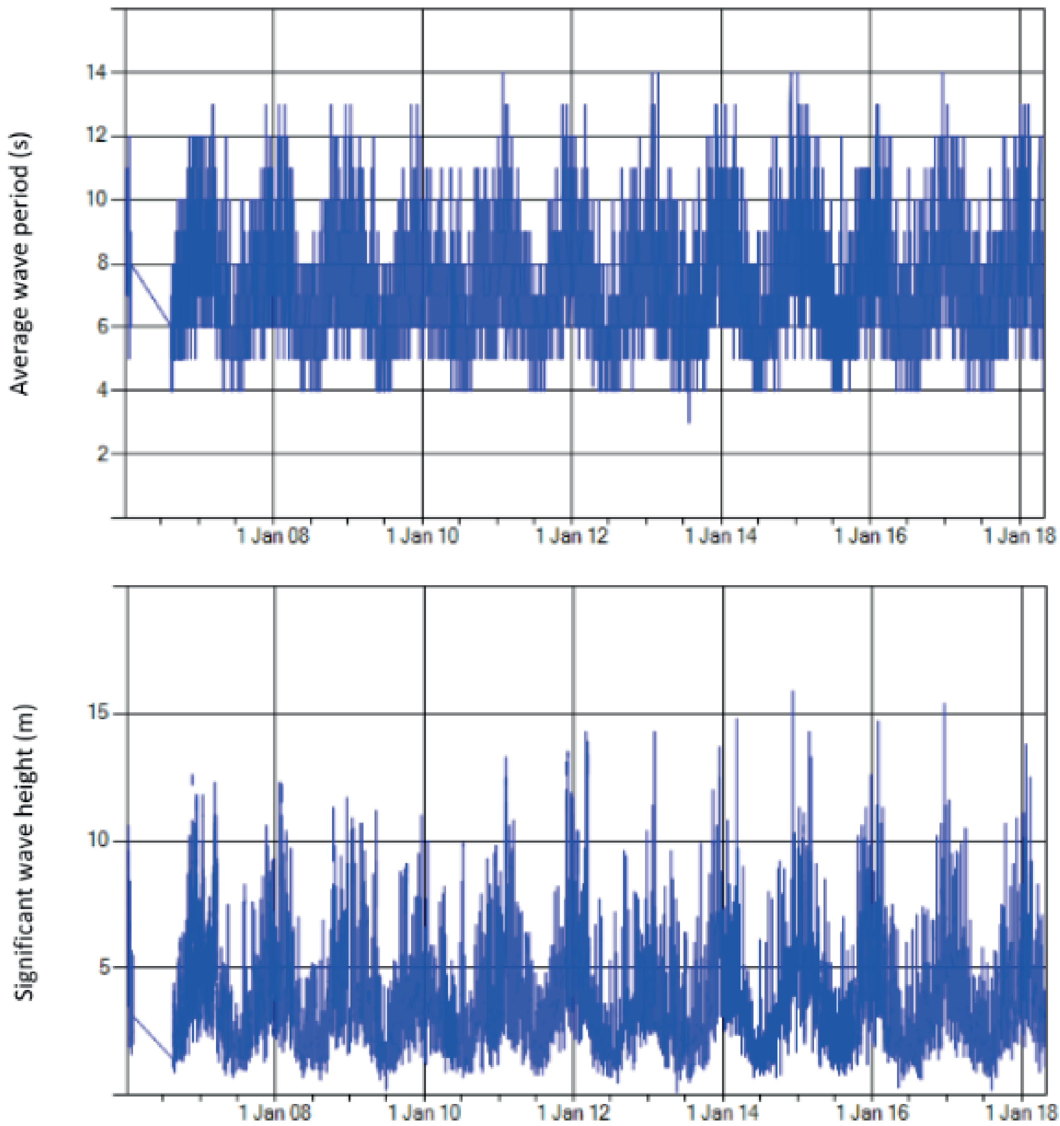

Figure 16. Wave data at the K5 buoy: significant wave height and average wave period.
(Source: Cefas (2018); © Crown Copyright 2018)

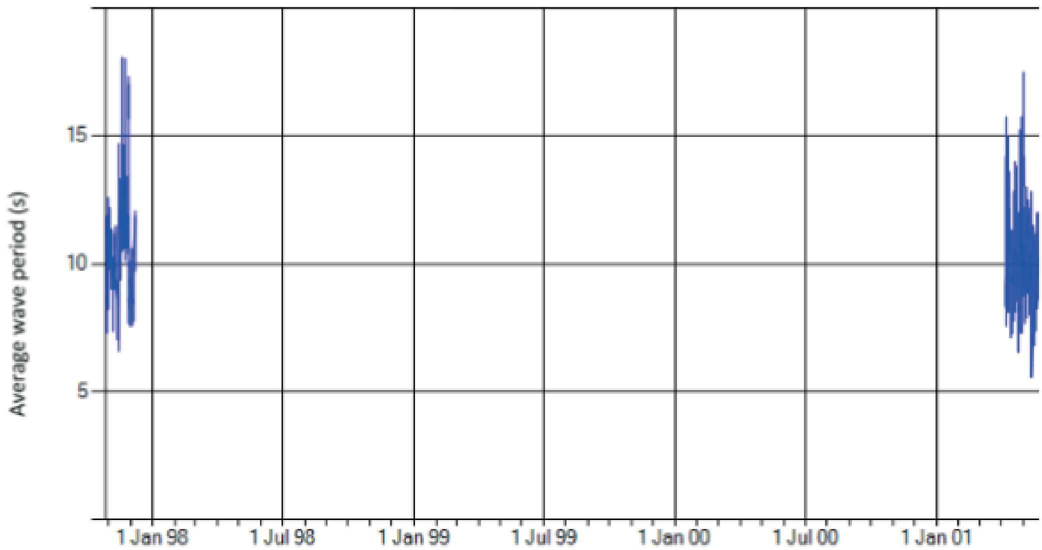

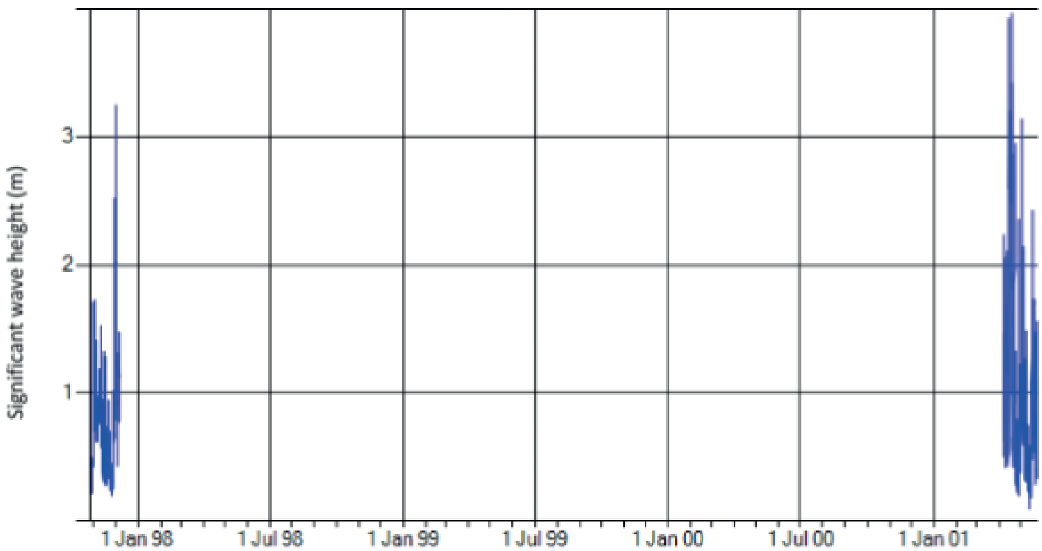

Figure 17. Historical wave data at Dounreay: significant wave height and average wave period. (Source: Cefas (2018); © Crown Copyright 2018)

Appendix C: Species data for Dounreay

Individual species data extracted from the HR Wallingford study are presented in the following table. The data were extracted to show the populace of the marine regions adjacent to Dounreay. Dounreay is located on the border of two nominal but large marine regions (namely the North Atlantic Ocean and the North Sea), so the populace reflects species from both regions; however, there are only small differences between the two regions.

The table is intended to give an example of the types of data that can be collected. For clarity, some columns of data have been omitted. It is reiterated that the data do become obsolete with time (because observable changes in species populations can become significant in that order of time); thus, the data may have changed since the exercise was undertaken in 2016. The reader is encouraged to use the latest information from the References section.

Note that since the HR Wallingford study was undertaken, the Marine Life Information Network (MarLIN) website has undergone reorganisation and the original web links no longer work; however, the MarLIN website (*MarLIN, 2018*) may be navigated to find the latest information.

Table 15. Extract from detailed marine species database developed for this project by HR Wallingford. Table focuses on species that could be observed at the Dounreay site and is a snapshot of species in 2016.

ID	Family	Genus	Species	Common names	Species type	Spawning	Life expectancy	Growth rate	Supplemental information	Web reference
1	Ulmaridae	Aurelia	aurita	Moon jellyfish	'Mobile'	Late winter/ early spring	8 months as medusa	Up to 5 mm per day	Clogging is more likely with small individuals in a dense bloom, than large individuals, which tend to be more dispersed	*https://www.marlin.ac.uk/species/detail/2089*
3	Rhiszostomatidae	Rhizostoma	pulmo	Barrel jellyfish	'Mobile'					*https://www.marlin.ac.uk/species/detail/2027*
4	Cyaneidae	Cyanea	capillata	Lion's mane jellyfish	'Mobile'					*https://www.marlin.ac.uk/species/detail/2090*
5	Cyaneidae	Cyanea	lamarckii	Blue jellyfish	'Mobile'					*https://www.marlin.ac.uk/species/detail/2025*
6	Pleurobrachiidae	Pleurobrachia	pileus	Sea gooseberry	'Mobile'	April to September	0	4 mm per month	Vertical migration during summer months only	*https://www.marlin.ac.uk/species/detail/2050*
8	Mytilidae	Mytilus	edulis	Blue mussel, edible mussel	Coloniser		18 years	2 mm per month		*https://www.marlin.ac.uk/species/detail/1421*
11	Ascidiiae	Ascidia	mentula	Red sea squirt	Coloniser	Year round	8 years		Prefers shaded areas for settlement	*https://www.marlin.ac.uk/species/detail/8*
12	Ascidiiae	Ascidiella	scabra		Coloniser	All year	2 years			*https://www.marlin.ac.uk/species/detail/1823*
13	Cionidae	Ciona	intestinalis	Common sea squirt	Coloniser	April to July				*https://www.marlin.ac.uk/species/detail/1369*
15	Alariaceae	Alaria	esculenta	Dabberlocks, wing kelp, murlins	'Mobile' and Coloniser		5 years	20 cm per month		*https://www.marlin.ac.uk/species/detail/1291*
21	Chordaceae	Chorda	filum	Dead man's bootlace	'Mobile' and Coloniser		Annual – spores overwinter	17 cm per month		*https://www.marlin.ac.uk/species/detail/1366*
24	Fucaceae	Cystoseira	baccata	Bushy berry wrack	'Mobile' and Coloniser					*http://www.marinespecies.org/aphia.php?p=taxdetails&id=145507*
26	Fucaceae	Cystoseira	nodicaulis	Rainbow wrack	'Mobile' and Coloniser					*http://www.marinespecies.org/aphia.php?p=taxdetails&id=145526*
27	Fucaceae	Cystoseira	tamariscifolia	Bushy rainbow wrack	'Mobile' and Coloniser					*http://www.marinespecies.org/aphia.php?p=taxdetails&id=145536*
31	Fucaceae	Fucus	guiryi	Guiry's wrack	'Mobile' and Coloniser					*http://www.marinespecies.org/aphia.php?p=taxdetails&id=624602*
35	Fucaceae	Fucus	vesiculosus	Bladder wrack	'Mobile' and Coloniser		5 years	2 cm per month		*https://www.marlin.ac.uk/species/detail/1330*
37	Sargassacae	Halidrys	siliquosa	Podweed, sea oak	'Mobile' and Coloniser					*https://www.marlin.ac.uk/species/detail/1450*

Appendix C: Species data for Dounreay

ID	Family	Genus	Species	Common names	Species type	Spawning	Life expectancy	Growth rate	Supplemental information	Web reference
39	Laminariaceae	Laminaria	digitata	Kelp	'Mobile' and Coloniser		10 years	40 cm per month		*https://www.marlin.ac.uk/species/detail/1386*
41	Laminariaceae	Laminaria	hyperborea	Kelp, mayweed, tangle	'Mobile' and Coloniser		20 years	30 cm per month		*https://www.marlin.ac.uk/species/detail/1309*
43	Laminariaceae	Laminaria	ochroleuca		'Mobile' and Coloniser					*https://www.marlin.ac.uk/species/detail/1838*
45	Fucaceae	Pelvetia	canaliculata	Channeled wrack	'Mobile' and Coloniser		5 years	0.3 cm per month		*https://www.marlin.ac.uk/species/detail/1342*
51	Sargassacae	Sargassum	muticum	Japweed, wireweed	'Mobile' and Coloniser			120 cm per month	Invasive species	*https://www.marlin.ac.uk/species/detail/1477*
53	Alariaceae	Undaria	pinnatifida	Wakame, Asian kelp	'Mobile' and Coloniser		14 months	30 cm per month	Invasive species	*https://www.marlin.ac.uk/species/detail/2142*
55	Ulvacea	Ulva	lactuca	Sea lettuce	'Mobile' and Coloniser		4 months			*https://www.marlin.ac.uk/species/detail/1467*
58	Clupeidae	Sprattus	sprattus	Sprat	'Mobile'	March to August	4 years	6 mm per month		*https://www.marlin.ac.uk/species/detail/82*
59	Ammodytidae	Ammodytes	marinus	Lesser sand eel	'Mobile'	February to March				*https://www.marlin.ac.uk/species/detail/59*
60	Syngnathidae	Syngnathus	spp	Pipe fish	'Mobile'				Without knowing specific species, it is difficult to provide authoritative information	
61	Actiniidae	Anemonia	viridis	Snakelocks anemone	Coloniser					*https://www.marlin.ac.uk/species/detail/1415*
62	Actiniidae	Urticina	felina	Dahlia anemone	Coloniser		50 years			*https://www.marlin.ac.uk/species/detail/1392*
63	Balanidae	Balanus	balanus	Acorn barnacle	Coloniser	February to April	6 years			*https://www.marlin.ac.uk/species/detail/2222*
64	Balanidae	Balanus	crenatus	Acorn barnacle	Coloniser	February to September	18 months	4.4 mm per month		*https://www.marlin.ac.uk/species/detail/1381*
66	Clavidae	Cordylophora	caspia	Freshwater hydroid	Coloniser	June to August	1 year	0.001 cm per hour		*https://www.marlin.ac.uk/species/detail/1511*
67	Metridiidae	Metridium	senile	Plumose anemone	Coloniser		20 years	9 cm per month		*https://www.marlin.ac.uk/species/detail/1185*
70	Sabellariidae	Sabellaria	spinulosa	Ross worm	Coloniser		5 years		Preferred substrate is shell and cobbles	*https://www.marlin.ac.uk/species/detail/1133*

Appendix C: Species data for Dounreay

ID	Family	Genus	Species	Common names	Species type	Spawning	Life expectancy	Growth rate	Supplemental information	Web reference
71	Serpulidae	Filograna	implexa	Filigree worm	Coloniser					*https://www.marlin.ac.uk/species/detail/20*
73	Serpulidae	Pomatoceros	triqueter	Keeled tubeworm	Coloniser				Invasive species	
74	Zosteraceae	Zostera	marina	Sea grass	'Mobile'		50 years	20 cm per month		*https://www.marlin.ac.uk/habitats/detail/257*
75	Austrobalanidae	Austrominius	modestus	Australasian barnacle	Coloniser					*https://www.marlin.ac.uk/species/detail/1771*
76	Bougainvilliidae	Bougainvillia	muscus	Hydroid	'Mobile' and Coloniser					
77	Chthamalidae	Chthamalus	stellatus	Poli's stellate barnacle	Coloniser					*https://www.marlin.ac.uk/species/detail/1323*
78	Moronidae	Dicentrarchus	labrax	Sea bass	'Mobile'	December to February	30 years		Only juveniles are likely to impinge on water intakes	*https://www.marlin.ac.uk/species/detail/2127*
79	Campanulariidae	Obelia	spp	Hydroid	'Mobile' and Coloniser				Without knowing specific species, it is difficult to provide authoritative information	
80	Patellidae	Patella	vulgata	Common limpet	Coloniser					*https://www.marlin.ac.uk/species/detail/1371*
81	Bangiaceae	Porphyra	umbilicalis	Purple laver	'Mobile' and Coloniser		1 year			*https://www.marlin.ac.uk/species/detail/1463*
82	Tubulariidae	Tubularia	indivisa	Oaten pipes hydroid	Coloniser		1 year			*https://www.marlin.ac.uk/species/detail/1967*

LC 0064_18CS2